AMS subject classifications. 34B45 Boundary value problems on graphs and networks, 05C21 Flows in graphs, 35L40 First-order hyperbolic systems, 35L60 Nonlinear first-order hyperbolic equations

Key words. Stationary states, Isothermal Euler equations, z-Factor, Compressibility factor, Real gas, Network, Node conditions, Gas transport, Gas networks

The final publication is available at Springer via http://dx.doi.org/10.1007/s40314-016-0383-z

NETWORKS OF PIPELINES FOR GAS WITH NONCONSTANT COMPRESSIBILITY FACTOR: STATIONARY STATES *

MARTIN GUGAT†, RÜDIGER SCHULTZ‡, AND DAVID WINTERGERST†

Abstract. For the management of gas transportation networks, it is essential to know how the stationary states of the system are determined by the boundary data. The isothermal Euler equations are an accurate pde-model for the gas flow through each pipe. A compressibility factor is used to model the nonlinear relationship between density and pressure that occurs in real gas in contrast to ideal gas. The gas flow through the nodes is governed by algebraic node conditions that require the conservation of mass and the continuity of the pressure. We examine networks that are described by arbitrary finite graphs and show that for suitably chosen boundary data, subsonic stationary states exist and are uniquely determined by the boundary data. Our construction of the stationary states is based upon explicit representations of the stationary states on each single pipe that can easily be evaluated numerically. We also use the monotonicity properties of these states as functions of the boundary data.

1. Introduction. Pipeline networks for gas transportation are an important part of the infrastructure. The 1-d isothermal Euler equations are a model for the flow that is motivated by the principles of continuum mechanics. In [Gugat et al., 2015], we have analyzed the stationary states for this model on certain pipeline networks for the case of an ideal gas where the sound speed is constant. In more realistic models for the gas—so-called real gas—the sound speed is not constant, but depends on the pressure of the gas. Therefore, a compressibility factor z depending on the pressure is introduced. For the ideal gas this factor is equal to one. In this paper, we consider a z-factor that depends in an affine linear way on the pressure. For single pipes, the corresponding states have also been discussed in [Schmidt et al., 2014], but here we provide a more explicit representation.

We study the stationary states in networks with real gas. The analysis of the stationary states is essential for the management of the pipeline systems, since usually supply and demand remain constant at certain time intervals. Also, the methods to evaluate gas network capacities presented in [Koch et al., 2015] are based upon stationary states.

* The final publication is available at Springer via http://dx.doi.org/10.1007/s40314-016-0383-z We would like to thank the reviewers for their helpful constructive comments. This work was supported by DFG in the framework of the Collaborative Research Centre CRC/Transregio 154, Mathematical Modelling, Simulation and Optimization Using the Example of Gas Networks, project C03, B05 and A05.

†Martin Gugat, martin.gugat@fau.de, David Wintergerst, david.wintergerst@fau.de
Friedrich-Alexander-Universität Erlangen-Nürnberg (FAU)
Department Mathematik, Cauerstr. 11
91058 Erlangen, Germany

‡Rüdiger Schultz,ruediger.schultz@uni-due.de
Universität Duisburg-Essen
Fakultät für Mathematik, Campus Essen, Thea-Leymann-Strasse 9
45127 Essen, Germany

While in [Gugat et al., 2015], only certain pipeline networks have been considered, in this paper, we present general results that are valid for networks that are given by arbitrary finite graphs. The analysis of networked systems of hyperbolic balance laws has received a lot of attention recently (see [Bressan et al., 2014]).

The optimal control of gas pipeline networks has been considered in several studies, for example [Colombo et al., 2009] and [Gugat and Herty, 2011]. An essential effect in the pipeline flow is the pressure loss in the gas along the pipe. This effect is modeled by a friction term in the pde and is typical for balance laws. In the case of conservation laws that appear for example in the context of traffic flow models (see [Garavello, 2009]) such a term does not appear. For the case without friction, the p-system has been studied in [Colombo and Marcellini, 2010]. In [Reigstad, 2014], numerical models for isothermal junction flow without friction term are presented. The flow through the pipe junctions in the network is governed by a system of algebraic node conditions. The conservation of mass yields the Kirchhoff condition. Moreover, it is assumed that the gas density at the junctions is the same at all adjacent pipes. The well-posedness of general networked systems of balance laws systems is studied in [Gugat et al., 2012]. Mixed integer models for the stationary case of gas network optimization have been considered in [Martin et al., 2006] and [Koch et al., 2015]. In [Ríos-Mercado et al., 2002] the flow system on networks was successfully solved independently for a simplified model, the so-called Weymouth approximation (see Sect. 3.1). The results are however not applicable for our model, because pressure and flow do not decouple in the way that is used in the proof of the main result in [Ríos-Mercado et al., 2002]. Recent results on solutions of the p-system are given in [Bressan et al., 2015], where it is pointed out that for general pressure laws the total variation of the solution can become arbitrarily large. For the pressure law that we consider in this paper, Bakhvalov's condition holds which implies that the p-system for barotropic gas has a global entropy weak solution with uniformly bounded total variation; see [Bressan et al., 2015] and [Bakhvalov, 1970].

This paper is organized as follows. In Sect. 2 we state the isothermal Euler equations. In Sect. 3 we consider the stationary states on the pipes of our network. A comparison with the Weymouth equation that is often used as a simple model for the stationary states is given in Sect. 3.1. The monotonicity properties of the solution with respect to the given boundary values in each single pipe allow the construction of stationary states on networks. The flow through the junctions of the network is governed by Kirchhoff's coupling conditions, which yield the conservation of mass and the continuity of pressure. In Sect. 4 three small graphs are treated: a tree (Sect. 4.1), a network with two parallel pipes (Sect. 4.2) and a diamond-shaped graph (Sect. 4.3). These three graphs are examples for the case of a graph with no circles, a graph with one circle and a graph with two circles. In all three cases, an explicit approach to construct a solution is given. In Sect. 4.4 the case of an arbitrary finite connected graph is considered and the existence and uniqueness of a subsonic solution is shown for appropriately chosen boundary data. Conclusions are given in Sect. 5.

2. The Isothermal Euler Equations. Let a finite graph $G = (V, E)$ of a pipeline network be given, where V denotes the set of vertices and E denotes the set of edges. Each edge $e \in E$ corresponds to a pipe in the network. Let $D^e > 0$ denote the corresponding pipe diameter and $\lambda^e_{\rm fric}(x) > 0$ the space-dependent Lipschitz continuous friction coefficient.

Define $\theta^e(x) = \frac{\lambda^e_{\rm fric}(x)}{D^e}$. Let ρ^e denote the gas density, p^e the pressure and q^e the

mass flow rate. Let $\alpha^e \in (-0.9,\, 0)$ and

$$z^e(p^e) = 1 + \alpha^e\, p^e \tag{2.1}$$

the compressibility factor. We use the state equation for real gas

$$p^e = RT^e z^e(p^e)\rho^e,$$

where T^e is the temperature and R is the specific gas constant. We study the isothermal Euler equations for horizontal pipes

$$\begin{cases} \rho^e_t + q^e_x = 0, \\ q^e_t + \left(p^e + \dfrac{(q^e)^2}{\rho^e}\right)_x = -\dfrac{1}{2}\theta^e \dfrac{q^e|q^e|}{\rho^e} \end{cases}$$

that govern the flow through a single pipe. In our analysis, the velocity $v^e = \frac{q^e}{\rho^e}$ and the Mach number $\frac{v^e}{c^e}$ appear, where $c^e > 0$ denotes the sound speed in the gas. We have

$$\left(\frac{1}{c^e}\right)^2 = \frac{\partial \rho^e}{\partial p^e}. \tag{2.2}$$

The case of an ideal gas that is $\alpha^e = 0$, has been considered in [Gugat et al., 2015]. Equation (2.1) is also stated in [Schmidt et al., 2014] as the model of the American Gas Association (AGA). It is sufficiently accurate within the network operating range (see [de Almeida et al., 2014]).

We consider the case of subsonic flow where the absolute value of the velocity of the gas is strictly less than the sound speed in the gas. This is the case that is relevant for gas transportation networks, because if the velocity of the gas in the pipelines is too large, vibrations of the pipes can develop and cause noise pollution. Moreover, excessive piping vibration can damage the system. Therefore, there are upper bounds for the velocity of the gas in the operation of gas pipelines. A detailed study of fluid-induced vibration of natural gas pipelines is given in [Zou et al., 2005].

3. The Stationary States in the Pipes. Each edge $e \in E$ of the network graph corresponds to an interval of the length $L^e > 0$ with the boundary points $x = 0$ and $x = L^e$. In this section, we determine the stationary states on these intervals. The first equation in the isothermal Euler equations implies that for every stationary state, the flow rate q^e is constant. The pressure p^e satisfies an ordinary differential equation on $[0,\, L^e]$. To derive this equation, we use the state equation for real gas

$$\frac{1}{\rho^e} = RT^e\left(\alpha^e + \frac{1}{p^e}\right),$$

to eliminate ρ^e from the second equation in the isothermal Euler equations. Since q^e is constant for stationary states, we get the differential equation

$$\left(1 - \left(\frac{q^e}{p^e}\right)^2 RT^e\right) p^e_x = -\frac{1}{2}\theta^e q^e|q^e|\left(\alpha^e + \frac{1}{p^e}\right) RT^e. \tag{3.1}$$

We consider classical stationary states. The velocity is given by

$$v^e = \frac{q^e}{\rho^e} = RT^e q^e\left(\alpha^e + \frac{1}{p^e}\right).$$

Define η^e as the square of the Mach number

$$\eta^e = \left(\frac{v^e}{c^e}\right)^2 = (v^e)^2 \left(\frac{1}{c^e}\right)^2. \tag{3.2}$$

Then, (2.2) implies that

$$\eta^e = \left(RT^e q^e \left(\alpha^e + \frac{1}{p^e}\right)\right)^2 \frac{1}{RT^e} \frac{1}{(1+\alpha^e p^e)^2} = RT^e \left(\frac{q^e}{p^e}\right)^2. \tag{3.3}$$

For the subsonic states that are relevant in the applications, we have $\eta^e < 1$. In (3.1), the factor in front of p_x^e is $(1-\eta^e)$, so it is clear that if η^e approaches 1, that is if the velocity approaches sound speed, a singularity in the derivative occurs.

To prepare the integration, we rewrite (3.1) in the form:

$$\left[\frac{1}{\alpha^e} + \left((q^e)^2 RT^e - \frac{1}{(\alpha^e)^2}\right)\frac{\alpha^e}{1+\alpha^e p^e} - \frac{(q^e)^2 RT^e}{p^e}\right] p_x^e = -\frac{1}{2} RT^e \theta^e q^e |q^e|.$$

With a constant C^e, by integration this yields the equation

$$\begin{aligned}&\frac{1}{\alpha} p^e + \left((q^e)^2 RT^e - \frac{1}{(\alpha^e)^2}\right) \ln(|1+\alpha^e p^e|) - (q^e)^2 RT^e \ln(p^e) \\ &\quad = C^e - \frac{1}{2} RT^e q^e |q^e| \int_{x_0}^{x} \theta^e(s)\, ds.\end{aligned}$$

To analyze the solution of (3.1), we need the following lemma, where the strictly increasing, differentiable and strictly convex auxiliary function F^e is introduced that can easily be evaluated numerically.

LEMMA 3.1. *For $p^e \in \left(0, \frac{1}{|\alpha^e|}\right)$, define the auxiliary function*

$$F^e(p^e) := \frac{1}{\alpha^e} p^e + \left((q^e)^2 RT^e - \frac{1}{(\alpha^e)^2}\right) \ln(|1+\alpha^e p^e|) - (q^e)^2 RT^e \ln(p^e). \tag{3.4}$$

Then, F^e is differentiable on $\left(0, \frac{1}{|\alpha^e|}\right)$ and

$$(F^e)'(p^e) = \frac{(p^e)^2 - (q^e)^2 RT^e}{p^e(1+\alpha^e p^e)}. \tag{3.5}$$

For subsonic flow (that is $\eta^e < 1$), we have $(p^e)^2 - (q^e)^2 RT^e > 0$; hence, F^e is strictly increasing on $\left(|q^e|\sqrt{RT^e}, \frac{1}{|\alpha^e|}\right)$. For the second derivative, we have

$$(F^e)''(p^e) = \frac{(p^e)^2 + (q^e)^2 RT^e (1+2\alpha^e p^e)}{(p^e)^2 (1+\alpha^e p^e)^2}. \tag{3.6}$$

Thus for subsonic flow, we have

$$(F^e)''(p^e) \geq \frac{2(q^e)^2 RT^e (1+\alpha^e p^e)}{(p^e)^2 (1+\alpha^e p^e)^2} > 0;$$

thus F^e is strictly convex on $\left(|q^e|\sqrt{RT^e}, \frac{1}{|\alpha^e|}\right)$. We have

$$\partial_{q^e} F^e(p^e) = 2q^e RT^e \ln\left(\left|\alpha^e + \frac{1}{p^e}\right|\right). \tag{3.7}$$

With the function F^e from Lemma 3.1, we can write the solution of (3.1) as

$$p^e(x) = (F^e)^{-1}\left(F^e(p_0^e) - \frac{1}{2}RT^e q^e|q^e|\int_{x_0}^{x}\theta^e(s)\,ds\right). \tag{3.8}$$

The decay of the pressure along the pipe is shown in Fig. 1, while the behavior of the pressure at the outlet for varied ingoing pressure p_0^e is illustrated in Fig. 2.

REMARK 1. *The inverse function $(F^e)^{-1}$ can be evaluated numerically with Newton's method. For a given $z > F(|q^e|\sqrt{RT^e})$, we define*

$$\varphi^e(y) := F^e(y) - z.$$

Finding a root of φ^e is equivalent to calculating $(F^e)^{-1}(z)$. Because F^e is strictly monotonously increasing on $\left(|q^e|\sqrt{RT^e}, \frac{1}{|\alpha^e|}\right)$ the same holds for φ^e. Additionally, we have

$$\varphi^e(|q^e|\sqrt{RT^e}) < 0 \quad \text{and} \quad \lim_{y \nearrow \frac{1}{|\alpha^e|}} F^e(y) = \infty.$$

This implies that we have a unique root $y^* \in \left(|q^e|\sqrt{RT^e}, \frac{1}{|\alpha^e|}\right)$. For each starting point $y_0 \in \left(y^*, \frac{1}{|\alpha^e|}\right)$, the Newton iteration

$$y_{n+1} = y_n - \frac{\varphi^e(y_n)}{(\varphi^e)'(y_n)}$$

generates a monotonously decreasing sequence that converges to y^*. This follows from the convexity of F^e, which implies the convexity of φ^e on $\left(|q^e|\sqrt{RT^e}, \frac{1}{|\alpha^e|}\right)$.

To determine the stationary states on a network, the sensitivities of $p^e(L^e)$ with respect to $p^e(0)$ and q^e are important. The following lemma gives explicit representations of the sensitivities.

LEMMA 3.2. *Consider subsonic flow, that is $(q^e)^2RT^e < (p^e)^2$. For $x \in [0,\, L^e]$, define*

$$p^e(x, q^e, p_0^e) = (F^e)^{-1}\left(F^e(p_0^e) - \frac{1}{2}RT^e q^e|q^e|\int_{x_0}^{x}\theta^e(s)\,ds\right), \tag{3.9}$$

where F^e is defined as in (3.4). Then, we have

$$\partial_{p_0^e} p^e(x, q^e, p_0^e) = \frac{(F^e)'\,(p_0^e)}{(F^e)'\,(p^e(x, q^e, p_0^e))} > 0, \tag{3.10}$$

$$\begin{aligned}\partial_{q^e} p^e(x, q^e, p_0^e) = {} & \frac{2q^e\,RT^e\,p^e(x,\,q^e,\,p_0^e)\,z^e(p^e(x,\,q^e,\,p_0^e))}{(p^e(x, q^e, p_0^e))^2 - (q^e)^2RT^e} \\ & \cdot\left[\ln\left(\tfrac{z^e(p_0)}{z^e(p^e(x,q^e,p_0^e))}\right) - \ln\left(\tfrac{p_0^e}{p^e(x,q^e,p_0^e)}\right) - \tfrac{1}{2}\operatorname{sign}(q^e)\int_{x_0}^{x}\theta^e(s)\,ds\right].\end{aligned} \tag{3.11}$$

Thus for $q^e = 0$, we have

$$\partial_{q^e} p^e(x, q^e, p_0^e) = 0$$

and for $q^e \neq 0$

$$\partial_{q^e} p^e(x, q^e, p_0^e) < 0.$$

Proof. Equation (3.10) follows from the definition of p^e and the the formula for the derivative of the inverse. We have

$$F^e(p^e(x, q^e, p_0^e)) = F^e(p_0^e) - \frac{1}{2} RT^e q^e |q^e| \int_{x_0}^{x} \theta^e(s)\, ds. \tag{3.12}$$

With (3.7), partial differentiation with respect to q^e yields

$$\begin{aligned}(F^e)'\,(p^e(x, q^e, p_0^e))\partial_{q^e} p^e(x, q^e, p_0^e) + \partial_{q^e} F^e(p^e(x, q^e, p_0^e)) = \\ \partial_{q^e} F^e(p_0^e) - RT^e |q^e| \int_{x_0}^{x} \theta^e(s)\, ds.\end{aligned}$$

Thus we have

$$\partial_{q^e} p^e(x, q^e, p_0^e) = \frac{\partial_{q^e} F^e(p_0^e) - \partial_{q^e} F^e(p^e(x, q^e, p_0^e)) - RT^e |q^e| \int_{x_0}^{x} \theta^e(s)\, ds}{F^{e\prime}(p^e(x, q^e, p_0^e))}.$$

This yields (3.11). ∎

Remark 2. *For practical applications one might be interested in a flow-dependent friction coefficient* $\theta^e(q^e)$ *(independent of* x*). Then the derivative* (3.11) *becomes*

$$\begin{aligned}\partial_{q^e} p^e(x, q^e, p_0^e) = \frac{2q^e\, RT^e\, p^e(x,\, q^e,\, p_0^e)\, z^e(p^e(x,\, q^e,\, p_0^e))}{(p^e(x, q^e, p_0^e))^2 - (q^e)^2 RT^e} \\ \cdot \left[\ln\left(\frac{z^e(p_0) p^e(x, q^e, p_0^e)}{z^e(p^e(x, q^e, p_0^e)) p_0^e}\right) - \tfrac{1}{2}\operatorname{sign}(q^e)\,\theta^e(q^e)x - \tfrac{1}{4}|q^e|\,\partial_{q^e}\theta^e(q^e)x\right].\end{aligned}$$

Most friction laws are decreasing in the flow. For an overview of different friction laws, see [Ghanbari et al., 2011]. For positive flow, a sufficient condition to ensure that the pressure at the end of the pipe remains decreasing in the flow can be given by

$$-\partial_{q^e}\theta^e(q^e)|q^e| < 2\theta^e(q^e).$$

This means the absolute value of the derivative of θ^e *has to be sufficiently small.* An important property of the pressure function is that it is decreasing in flow direction.

Lemma 3.3. *For subsonic flow* $p^e > |q^e|\sqrt{RT^e}$ *and* $p^e < \frac{1}{|\alpha^e|}$*, we have*

$$\operatorname{sign}(p_x^e(x, q^e, p_0^e)) = -\operatorname{sign}(q^e). \tag{3.13}$$

Proof. Consider Eq. (3.1). Because the flow is subsonic, the sign of the term $1 - \left(\frac{q^e}{p^e}\right)^2 RT^e$ is positive, and because $p^e < \frac{1}{|\alpha^e|}$, the sign of $\alpha^e + \frac{1}{p^e}$ is also positive. This shows the claim. ∎

For the second space derivative, we get the following Lemma.

Lemma 3.4. *For subsonic flow* $p^e > |q^e|\sqrt{RT^e}$*, positive compressibility factor* $p^e < \frac{1}{|\alpha^e|}$ *and under the assumption of a constant friction factor* θ^e*, we have*

$$p_{xx}^e(x, q^e, p_0^e) < 0. \tag{3.14}$$

Proof. Implicit differentiation of (3.1) with respect to x yields

$$\left(1-\left(\frac{q^e}{p^e}\right)^2 RT^e\right)p^e_{xx}+\frac{2(q^e)^2RT^e}{(p^e)^3}(p^e_x)^2=\frac{1}{2}\theta^e q^e|q^e|\frac{p^e_x}{(p^e)^2}RT^e.$$

After reordering, we get

$$\left(1-\left(\frac{q^e}{p^e}\right)^2 RT^e\right)p^e_{xx}=\frac{(q^e)^2RT^e}{(p^e)^2}p_x\left(\frac{1}{2}\operatorname{sign}(q^e)\theta^e-2\frac{p^e_x}{p^e}\right).$$

Because the flow is subsonic, we have $1-\left(\frac{q^e}{p^e}\right)^2 RT^e>0$. The sign of p_x is $-\operatorname{sign}(q^e)$, which was stated in Lemma 3.3. This concludes the proof. ∎

Let us assume θ^e to be constant and view the solution on the interval $[0,L^e]$. This means that the evaluation of the integral term yields

$$\tfrac{1}{2}RT^eq^e|q^e|\int_0^{L^e}\theta^e(s)ds=\tfrac{1}{2}RT^eq^e|q^e|\theta^eL^e.$$

The sensitivity regarding the friction coefficient is of special interest if one assumes that it is uncertain.

LEMMA 3.5. *For subsonic flow $(q^e)^2RT^e<(p^e)^2$ and $p^e<\frac{1}{|\alpha^e|}$, the sensitivity regarding the roughness can be calculated by*

$$\partial_{\theta^e}p^e(L^e,q^e,p^e_0)=\frac{-\frac{1}{2}RT^eq^e|q^e|L^e}{(F^e)'\left(p^e(L^e,q^e,p^e_0)\right)}. \tag{3.15}$$

The sign is given by

$$\operatorname{sign}\left(\partial_{\theta^e}p^e(L^e,q^e,p^e_0)\right)=-\operatorname{sign}(q^e).$$

Proof. Differentiation of Eq. (3.12) and keeping in mind that neither F^e nor p^e_0 depend on θ^e lead to

$$\partial_{p^e}F^e(p^e)\,\partial_{\theta^e}p^e=-\tfrac{1}{2}RT^eq^e|q^e|\theta^eL^e.$$

Hence, (3.15) holds. ∎

It is useful to define a critical length up to which the existence of a solution is guaranteed. For this, we assume the friction coefficient θ^e to be constant.

COROLLARY 3.6. *Let $p^e_0\in\left(|q^e|\sqrt{RT^e},\frac{1}{|\alpha^e|}\right)$ be given. Define*

$$L^e_c=2\frac{F^e(p^e_0)-F^e\left(|q^e|\sqrt{RT^e}\right)}{RT^e|q^e|^2\theta^e}. \tag{3.16}$$

Then for all $0<x<L^e_c$ the solution $p^e(x,q^e,p^e_0)$ exists and is well defined.

Proof. It has to be shown that $p^e(x,q^e,p^e_0)\in\left(|q^e|\sqrt{RT^e},\frac{1}{|\alpha^e|}\right)$ holds. Lemma 3.3 shows that the p^e is decreasing in the flow direction. Consequently for positive

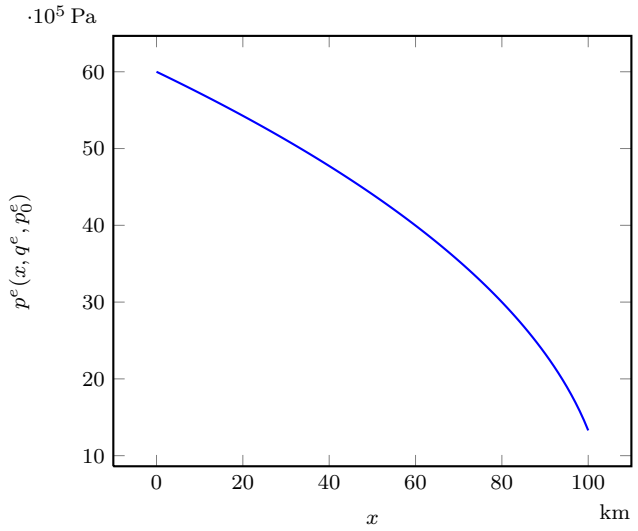

FIG. 1. *Pressure drop along the pipe for* $\theta^e = 0.014261$, $p_0^e = 60 \cdot 10^5$ Pa, $q^e = 453.1495\,\mathrm{kg\,m^{-2}\,s^{-1}}$

flow $q^e > 0$ the lower bound $|q^e|\sqrt{RT^e}$ is relevant. Keep in mind that F^e is increasing on the considered interval. This means that $p^e(x, q^e, p_0^e) > |q^e|\sqrt{RT^e}$ is equivalent to

$$F^e(p_0^e) - \tfrac{1}{2} RT^e q^e |q^e|\, \theta^e x > F^e\left(|q^e|\sqrt{RT^e}\right),$$

and because of $q^e > 0$, we have

$$x < 2\frac{F^e(p_0^e) - F^e\left(|q^e|\sqrt{RT^e}\right)}{RT^e q^e |q^e| \theta^e}.$$

The inequality holds for all $0 < x < L_c^e$ per definition of L_c^e. Now, we consider $q^e \leq 0$. Due to Lemma 3.3, we only need to show $p^e(x, q^e, p_0^e) < \frac{1}{|\alpha^e|}$ or equivalently

$$F^e(p_0^e) - \frac{1}{2} RT^e q^e |q^e| \theta^e x < \lim_{p \nearrow \frac{1}{|\alpha^e|}} F^e(p).$$

Since the right hand side is infinity, this inequality holds, which concludes the proof. ∎

It is also useful to be able to calculate the flow for given pressure values at both ends of the pipe. This compensatory flow will be needed in Sect. 4.3.

LEMMA 3.7. *Let* $p_0, p_1 \in \left(0, \frac{1}{|\alpha^e|}\right)$ *be the pressures given at both ends of the pipe and let the nonzero difference between* p_0 *and* p_1 *be small enough in the sense that*

$$0 < |p_0 - p_1| < p_0 + p_1 - 2\frac{\sqrt{\frac{1}{\alpha^e}(p_1 - p_0) - \frac{1}{(\alpha^e)^2} \ln\left(\frac{z^e(p_1)}{z^e(p_0)}\right)}}{\sqrt{\ln\left(\frac{p_1}{p_0}\frac{z^e(p_0)}{z^e(p_1)}\right) - \frac{1}{2}\operatorname{sign}(p_0 - p_1)\int_0^{L^e} \theta^e(s)ds}}. \tag{3.17}$$

Then the sign of the flow is determined by

$$\operatorname{sign}(q^e(p_0, p_1)) = \operatorname{sign}(p_0 - p_1) \tag{3.18}$$

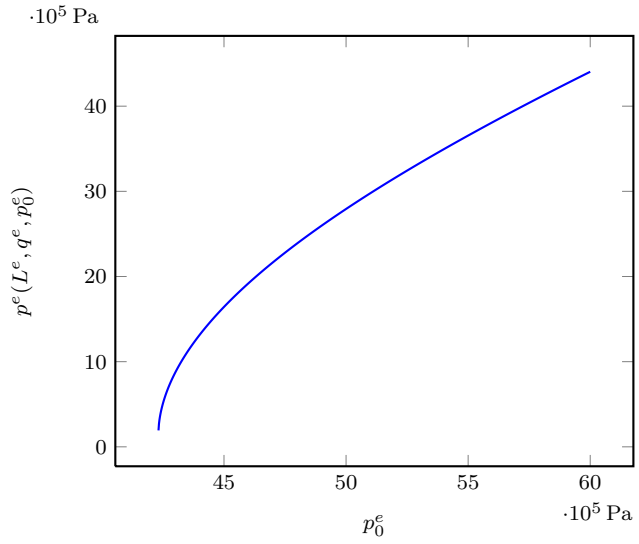

FIG. 2. *Pressure $p^e(L^e, q^e, \cdot)$ at the outflow as a function of different ingoing pressures for $\theta^e = 0.014261$, $L^e = 50\,\mathrm{km}$, $q^e = 453.1495\,\mathrm{kg\,m^{-2}\,s^{-1}}$*

and the flow can be calculated as

(3.19)
$$q^e(p_0, p_1) = \operatorname{sign}(p_0 - p_1)\sqrt{\frac{\frac{1}{\alpha^e}(p_1 - p_0) - \frac{1}{(\alpha^e)^2}\ln\left(\frac{z^e(p_1)}{z^e(p_0)}\right)}{RT^e\left[\ln\left(\frac{p_1}{p_0}\frac{z^e(p_0)}{z^e(p_1)}\right) - \frac{1}{2}\operatorname{sign}(p_0 - p_1)\int_0^{L^e}\theta^e(s)ds\right]}}.$$

For the case $p_0 = p_1$, the stationary flow is zero.

Proof. For simplicity, the arguments of q^e are suppressed in this proof. Let us for the moment assume subsonic flow, i.e., $|q^e|\sqrt{RT^e} < p^e$. We will show at the end of the proof that this inequality indeed holds. We start from Eq. (3.12) and retain

$$F^e(p_1) - F^e(p_0) = -\frac{1}{2}RT^e q^e|q^e|\int_0^{L^e}\theta^e(s)ds. \tag{3.20}$$

The monotonicity of F^e and $\int_0^{L^e}\theta^e(s)ds > 0$ leads to

$$\begin{aligned}\operatorname{sign}(q^e) &= -\operatorname{sign}(F^e(p_1) - F^e(p_0))\\ &= -\operatorname{sign}(p_1 - p_0)\\ &= \operatorname{sign}(p_0 - p_1).\end{aligned}$$

The definition of F^e can be used in (3.20) to obtain

$$\begin{aligned}&\frac{1}{\alpha^e}p_1 + \left((q^e)^2RT^e - \frac{1}{(\alpha^e)^2}\right)\ln(1 + \alpha^e p_1) - (q^e)^2RT^e\ln(p_1)\\ &- \frac{1}{\alpha^e}p_0 - \left((q^e)^2RT^e - \frac{1}{(\alpha^e)^2}\right)\ln(1 + \alpha^e p_0) + (q^e)^2RT^e\ln(p_0)\\ &\quad = -\frac{1}{2}RT^e\operatorname{sign}(q^e)(q^e)^2\int_0^{L^e}\theta^e(s)ds,\end{aligned}$$

which is equivalent to

$$\frac{1}{\alpha^e}(p_1-p_0)-\frac{1}{(\alpha^e)^2}\ln\left(\frac{1+\alpha^e p_1}{1+\alpha^e p_0}\right)$$
$$=-\frac{1}{2}RT^e\operatorname{sign}(q^e)(q^e)^2\int_0^{L^e}\theta^e(s)ds+(q^e)^2RT^e\left[\ln\left(\frac{p_1}{p_0}\right)-\ln\left(\frac{1+\alpha^e p_1}{1+\alpha^e p_0}\right)\right].$$

Because $-\operatorname{sign}(q^e)=\operatorname{sign}\left(\ln\left(\frac{p_1}{p_0}\right)\right)=-\operatorname{sign}\left(\ln\left(\frac{1+\alpha^e p_1}{1+\alpha^e p_0}\right)\right)$, we get

$$RT^e\left[\ln\left(\frac{p_1}{p_0}\right)-\ln\left(\frac{1+\alpha^e p_1}{1+\alpha^e p_0}\right)\right]-\frac{1}{2}\operatorname{sign}(p_0-p_1)RT^e\int_0^{L^e}\theta^e(s)ds\neq 0$$

and hence (3.19) holds. Now the inequality $\min\{p_0,p_1\}>|q^e|\sqrt{RT^e}$ remains to be shown. It follows from assumption (3.17). Because

$$\min\{p_0,p_1\}=\frac{p_0+p_1-|p_0-p_1|}{2},$$

we have

$$\min\{p_0,p_1\}>\frac{\sqrt{\frac{1}{\alpha^e}(p_1-p_0)-\frac{1}{(\alpha^e)^2}\ln\left(\frac{z^e(p_1)}{z^e(p_0)}\right)}}{\sqrt{\ln\left(\frac{p_1}{p_0}\frac{z^e(p_0)}{z^e(p_1)}\right)-\frac{1}{2}\operatorname{sign}(p_0-p_1)\int_0^{L^e}\theta^e(s)ds}}$$

$$=|q^e|\sqrt{RT^e}.\qquad\square$$

One can show the intuitive monotonicity properties of q^e, which are especially important for solutions on networks that will be considered later.

LEMMA 3.8. *Under the assumptions of Lemma 3.7, the derivatives of q^e satisfy*

$$\partial_{p_0}q^e(p_0,p_1)>0,$$
$$\partial_{p_1}q^e(p_0,p_1)<0.$$

Proof. Derivation of Eq. (3.20) with respect to p_0 leads to

$$RT^e\int_0^{L^e}\theta^e(s)\,ds\cdot\operatorname{sign}(q^e)q^e\partial_{p_0}q^e=(F^e)'(p_0)$$
$$\partial_{p_0}q^e=\frac{(F^e)'(p_0)}{RT^e|q^e|\int_0^{L^e}\theta^e(s)\,ds}.$$

Analogously, derivation with respect to p_1 yields

$$RT^e\int_0^{L^e}\theta^e(s)\,ds\cdot\operatorname{sign}(q^e)q^e\partial_{p_1}q^e=-(F^e)'(p_1)$$
$$\partial_{p_1}q^e=-\frac{(F^e)'(p_1)}{RT^e|q^e|\int_0^{L^e}\theta^e(s)\,ds}.\qquad\square$$

3.1. Comparison to the Weymouth equation. In this section, we compare the commonly used Weymouth equation (see [Schroeder Jr et al., 2010]) for the pressure loss with the solutions of Sect. 3. Once again, we assume the friction coefficient θ^e to be constant in x. The pressure function in the Weymouth equation has the form

$$p^e_{\text{weymouth}}(x, q^e, p^e_0) = \sqrt{(p^e_0)^2 - \theta^e x\,(c^e)^2 q^e |q^e|}, \tag{3.21}$$

where the sound speed is given by $(c^e)^2 = RT^e z^e_m$ for a constant compressibility factor z^e_m. We look at two different approaches for choosing the constant compressibility factor. First, the classical approach with an a priori estimate based on the initial pressure and, second, the optimal fit based on an exact fit of the ode solutions at both ends of an edge. Throughout this section, we assume that $q^e > 0$.

3.1.1. Initial value estimate. A constant approximation for the compressibility factor can be gained by the evaluation at p^e_0. In this case,

$$z^e_m = z(p^e_0) = 1 + \alpha p^e_0.$$

Using the initial guess, one retains $z^e_m = z(p^e_0) = 0.852$ in the example presented in Fig. 3. Since the value of both functions at $x = 0$ is identical, for $x \in [0, L^e]$ the error estimate

$$|p^e(x) - p^e_{\text{weymouth}}(x)| \le \max_{\xi\in[0,x]} \left| \frac{\partial p^e}{\partial x}(\xi) - \frac{\partial p^e_{\text{weymouth}}}{\partial x}(\xi) \right| |x| \tag{3.22}$$

holds. The derivative $\frac{\partial p^e_{\text{weymouth}}}{\partial x}(\omega)$ is given by

$$\frac{\partial p^e_{\text{weymouth}}}{\partial x}(\omega) = -\frac{\theta^e}{2} \frac{(c^e)^2 q^e |q^e|}{p^e_{\text{weymouth}}(\omega)},$$

and the derivative $\frac{\partial p^e}{\partial x}(\xi)$ is given by

$$\frac{\partial p^e(\xi)}{\partial x} = -\frac{1}{2} RT^e \theta^e q^e |q^e| \frac{p^e(\xi)(1 + \alpha p^e(\xi))}{(p^e(\xi))^2 - (q^e)^2 RT^e}.$$

This can be seen from Eq. (3.1). Further estimation of (3.22) yields

$$\begin{aligned} |p^e(x) - p^e_{\text{weymouth}}(x)| &\le \left(\left| \frac{\partial p^e}{\partial x}(x) \right| + \left| \frac{\partial p^e_{\text{weymouth}}}{\partial x}(x) \right| \right) x \\ &\le \left(\left| \frac{\partial p^e}{\partial x}(L^e) \right| + \left| \frac{\partial p^e_{\text{weymouth}}}{\partial x}(L^e) \right| \right) x, \end{aligned} \tag{3.23}$$

where the negativity of the first derivative (3.13) and the concavity (3.14) were used. The behavior of the pressure and the error curve is shown in Fig. 3. The error plot also contains the error bound (3.23).

To compare the different models, we also want to make an optimal fit by choosing z^e_m such that the pressure values at both ends of the pipe match.

3.1.2. Optimal fit. For a given pipe length L^e and constant flow q^e, we use the optimal z^e_m in the sense that $p^e_{\text{weymouth}}(L^e, q^e, p^e_0) = p^e(L^e, q^e, p^e_0)$ and analyze the

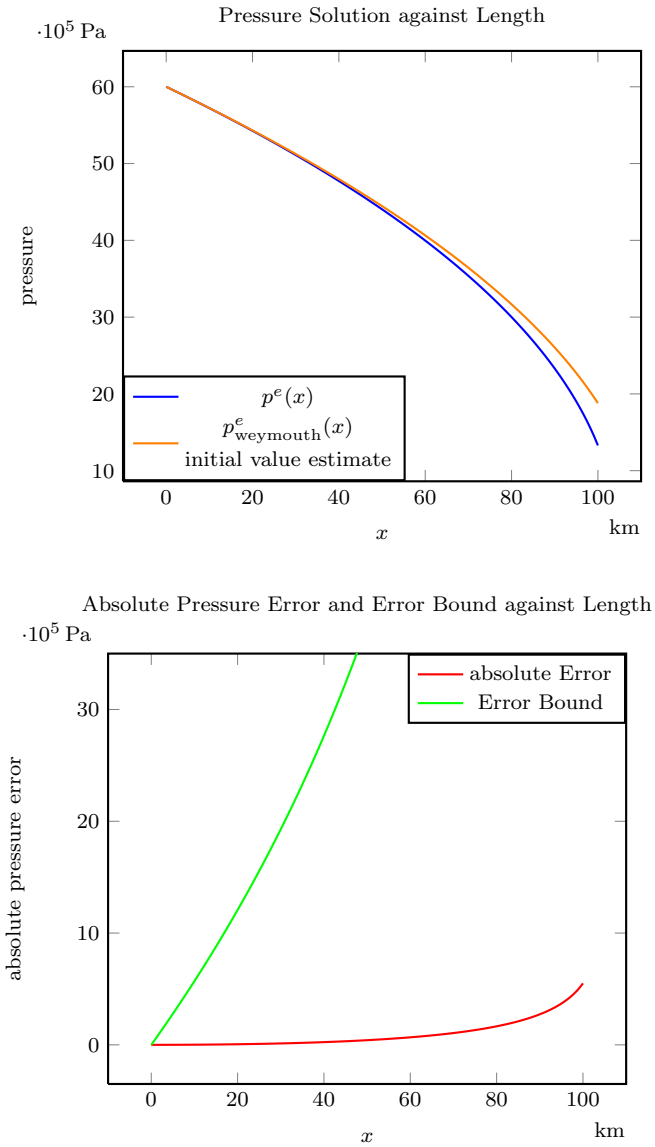

FIG. 3. *Pressure solution and error plot for* $\theta^e = 0.014261$, $L^e = 100\,\text{km}$, $p_0^e = 60 \cdot 10^5\text{Pa}$, $q^e = 453.1495\,\text{kg}\,\text{m}^{-2}\,\text{s}^{-1}$.

error for $x \in [0, L^e]$. We suppress the arguments q^e and p_0^e in the pressure function. With the length L^e inserted, Eq. (3.21) can be rewritten as

$$z_m^e = \frac{(p_0^e)^2 - \left(p^e_{\text{weymouth}}(L^e)\right)^2}{\theta^e L^e R T^e q^e |q^e|}.$$

For $p^e_{\text{weymouth}}(L) = p^e(L)$, we retain

$$z_m^e = \frac{(p_0^e)^2 - (p^e(L^e))^2}{\theta^e L^e R T^e q^e |q^e|}.$$

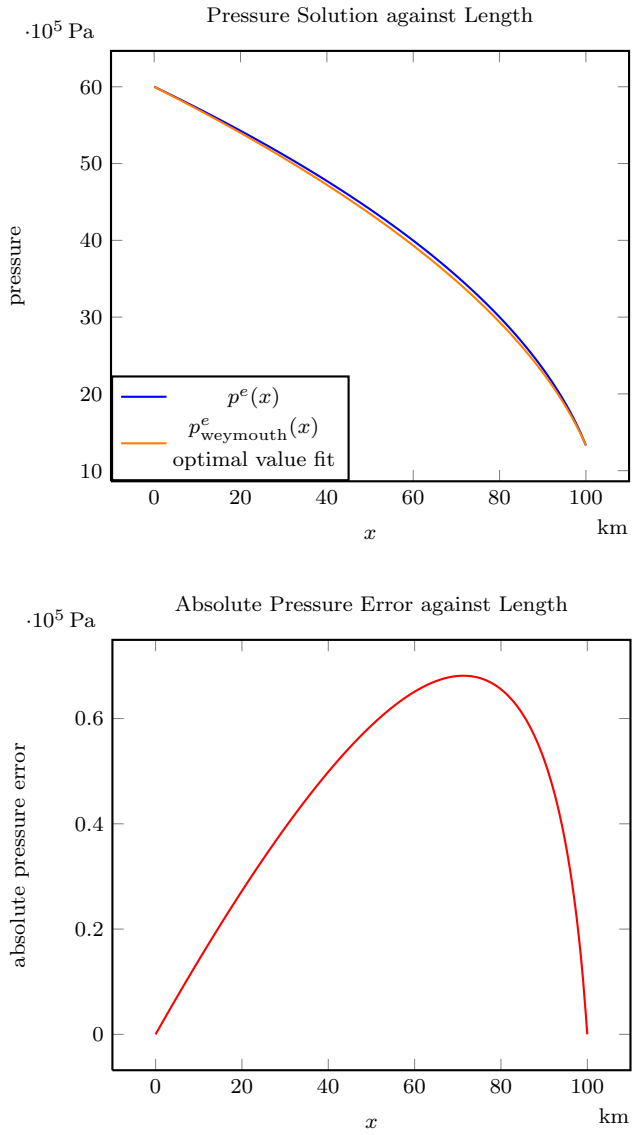

FIG. 4. *Pressure solution and error plot for* $\theta^e = 0.014261$, $L^e = 100\,\text{km}$, $p_0^e = 60 \cdot 10^5\text{Pa}$, $q^e = 453.1495\,\text{kg}\,\text{m}^{-2}\,\text{s}^{-1}$.

This yields

$$p^e_{\text{weymouth}}(x) = \sqrt{p_0^e - \frac{x}{L}\left((p_0^e)^2 - \left(p^e(L^e)\right)^2\right)}.$$

Both the fitted Weymouth equation and the pressure solution for the nonconstant compressibility factor are visualized in Fig. 4 as well as the error between both models. In our example, the optimal value of the compressibility factor is given by $z_m = 0.85217$.

4. Stationary States on Networks. In this section, we use the solutions on a single pipe to construct solutions on networks with appropriate coupling conditions. The node conditions that determine the flow dynamics are given in [Banda et al., 2006] for the case that all pipes have the same diameter D^e. Let a finite connected directed graph $G = (V, E)$ be given. Each edge $e \in E$ of the graph corresponds to an interval $[0, L^e]$. At the vertices $v \in V$, the flow is governed by the node conditions that require the conservation of mass and the continuity of the pressure. Let $E_0(v)$ denote the set of edges that are incident to $v \in V$ and $x^e(v) \in \{0, L^e\}$ the end of the interval $[0, L^e]$ corresponding to the edge e that is adjacent to v.

Define

$$\sigma(e,v) := \begin{cases} -1 & \text{if} \quad x^e(v) = 0 \text{ and } \ e \in E_0(v), \\ 1 & \text{if} \quad x^e(v) = L^e \text{ and } \ e \in E_0(v), \\ 0 & \text{if} \quad e \notin E_0(v). \end{cases} \tag{4.1}$$

The incidence matrix $A \in \mathbb{R}^{|V|\times|E|}$ corresponding to G is defined by $A_{ij} = \sigma(e_j, v_i)$. Then for all $e, f \in E_0(v)$ continuity of the pressure means we have the equation

$$p^e(x^e(v)) = p^f(x^f(v)). \tag{4.2}$$

Moreover, for nodes with no prescribed boundary flow, we have the Kirchhoff condition

$$\sum_{e\in E_0(v)} \sigma(e,v)\,(D^e)^2\,q^e(x^e(v)) = 0. \tag{4.3}$$

For simplicity, we assume $(D^e)^2 = (D^f)^2$ for all $e, f \in E$. If we define the vector of outflows in all nodes by $b \in \mathbb{R}^{|V|}$ such that

$$b \in B := \Big\{ b \in \mathbb{R}^{|V|} : \sum_{v\in V} b_v = 0 \Big\},$$

the Kirchhoff conditions with prescribed boundary flows $b \in B$ can be written as

$$A\,q = b, \quad q \in \mathbb{R}^{|E|}.$$

REMARK 3. *The case of different diameters can be calculated as follows. The mass flows $m^e = \frac{\pi}{4}(D^e)^2 q^e$ satisfy $Am = b$ for properly chosen outflows b. In each evaluation of p^e, the argument q^e can be retained via $q^e = \frac{4}{\pi(D^e)^2} m^e$.*

4.1. Stationary states on trees. First, we consider the case of a network without circles, that is $\ker(A) = \{0_{|E|}\}$. For given outflows $b \in B$, the linear system of equations $Aq = b$ has a unique solution.

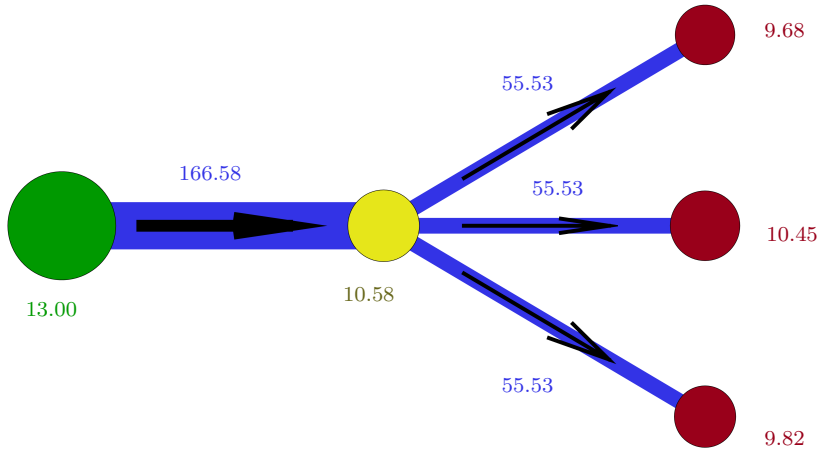

FIG. 5. *Solution of a tree network with pressure values an the nodes (in* 10^5 Pa*) and flow values at the edges (in* $\mathrm{kg\,s^{-1}m^{-2}}$*)*

LEMMA 4.1. *Let the outflows* $b \in B$ *and a pressure* $p_0 \in \left(|b_{v_0}|\sqrt{RT^e}, \frac{1}{|\alpha^e|}\right)$ *in* v_0 *be given, where* $e \in E(v_0)$*. Furthermore, let the boundary flow rates* b *be small enough that the vector* q *solving* $Aq = b$ *has entries such that the functions* $p^e(x^e(v), \sigma(e,v)q^e, p_v^e)$ *are well–defined, i.e.,*

$$(q^e)^2 < \frac{\left(p^e(x^e(v), \sigma(e,v)q^e, p_v^e)\right)^2}{RT^e}$$

and

$$p^e(x^e(v), \sigma(e,v)q^e, p_v^e) < \frac{1}{|\alpha^e|}$$

for all v *incident to* e*.*
Then the boundary data determine a unique subsonic stationary network flow that satisfies (4.2) *and* (4.3) *and on each edge (3.9).*

Proof. As already stated, the flow system $Aq = b$ has a unique solution, which satisfies (4.3) by definition. The assumptions ensure the existence of classical solutions of the isothermal Euler equations on each pipe. Thus, for each node v, the pressure can be calculated by looking at the unique path between v_0 and v. Starting from v_0, Eq. (3.9) gives the pressure value in the second node v_1 on the path. This procedure can be iterated until v is reached. Hereby, we retain a pressure value in each node and the pair (p, q) is the desired solution. ∎

An example can be seen in Fig. 5. The radius of each circle scales with the pressure value in the corresponding node. The thickness of each line scales with the flow value of the corresponding edge.

4.2. Networks with two parallel pipes. Let us now consider a network with two parallel pipes (see Fig. 6). While in the case of a tree graph, the continuity of the pressure was not necessary to determine the flow rates, here the situation is different. The flow system $A\,q = b$ on its own does not have a unique solution anymore, but (4.2) helps to eliminate the additional degree of freedom. The edges and nodes are

enumerated from left to right with the upper middle edge e_2 and the lower middle edge e_3. We assume that all edges point from left to right. A vector spanning the kernel of A is given by $q_K = (0, 1, -1, 0)^T$. For a given boundary flow $b = (b_0, 0, 0, -b_0)^T, b_0 < 0$, a specific solution of the system is defined by $q_s = (-b_0, -b_0, 0, -b_0)^T$. Each solution of $Aq = b$ satisfies

$$q(\lambda) = q_s + \lambda q_K, \text{ for } \lambda \in \mathbb{R}.$$

Our goal is to find a $\lambda \in [b_0, 0]$, such that in node v_2 the pressure is continuous. The pressure p_0 in v_0 is fixed. We assume our boundary data to be chosen properly (see assumptions Lemma 4.1) such that the classical solutions of the ode (3.1) with zero slope exist. The flows to consider are such that $q^e \in [0, |b_0|]$. Let us define

$$\begin{aligned} p^{\text{red}}(\lambda) &:= p^{e_2}(L^{e_2}, q^{e_2}(\lambda), p_{v_1}), \\ p^{\text{blue}}(\lambda) &:= p^{e_3}(L^{e_3}, q^{e_3}(\lambda), p_{v_1}), \end{aligned}$$

where $p_{v_1} = p^{e_1}(L^{e_1}, -b_0, p_0)$ is the pressure in node v_1. We define the auxiliary function

$$H(\lambda) := p^{\text{red}}(\lambda) - p^{\text{blue}}(\lambda).$$

Because the functions p^{red} and p^{blue} are continuous, H is continuous. Furthermore, p^{red} monotonously decreases and p^{blue} monotonously increases with respect to λ. This follows from Lemma 3.2. Thus, H monotonously decreases. For $\lambda = b_0$, we get $q(b_0) = (-b_0, 0, -b_0, -b_0)^T$,

$$p^{\text{red}}(b_0) = p^{e_2}(L^{e_2}, 0, p_{v_1}) = p_{v_1}$$

and

$$\begin{aligned} p^{\text{blue}}(b_0) &= p^{e_3}(L^{e_3}, -b_0, p_{v_1}) \\ &< p^{e_3}(L^{e_3}, 0, p_{v_1}) = p_{v_1}. \end{aligned}$$

Hence, the inequality $H(b_0) > 0$ follows. For $\lambda = 0$, we get $q(0) = (-b_0, -b_0, 0, -b_0)$,

$$\begin{aligned} p^{\text{red}}(0) &= p^{e_2}(L^{e_2}, -b_0, p_{v_1}) \\ &< p^{e_2}(L^{e_2}, 0, p_{v_1}) = p_{v_1} \end{aligned}$$

and

$$p^{\text{blue}}(0) = p^{e_3}(L^{e_3}, 0, p_{v_1}) = p_{v_1}.$$

In this case, $H(0) < 0$ holds. Because H is continuous and monotonously decreases, Bolzano's intermediate value theorem implies that there exists a number $\lambda^* \in (b_0, 0)$, such that $H(\lambda^*) = 0$. This leads to the flow $q(\lambda^*)$, and the pressure values in the nodes can be easily constructed.

4.3. Solutions on a diamond graph. Now, we look at a diamond-shaped graph as it is drawn in Fig. 7. One difficulty is that the flow direction on the middle edge e_4 is not known a priori. We have the value p_0 in v_1 and a flow $b_0 < 0$ given. The vector of outflows is $b = (b_0, 0, 0, 0, 0, -b_0)$. We assume that the absolute value of b_0 is

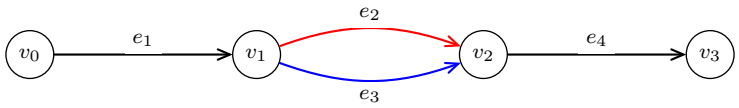

FIG. 6. *A graph with two parallel pipes*

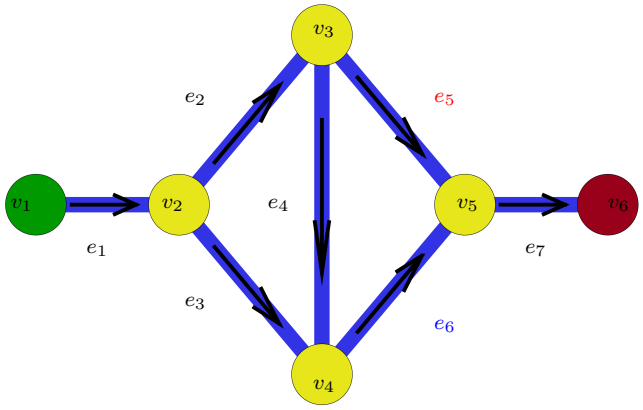

FIG. 7. *A diamond graph; source: green, inner nodes: yellow, sink: red*

sufficiently small to guarantee that the q^e that solve $Aq = b$ and fulfil $q^e \in [-|b_0|, |b_0|]$ are small enough in the sense that

$$(q^e)^2 < \frac{(p^e(x^e(v), \sigma(e,v)q^e, p_v^e))^2}{RT^e},$$

and

$$p^e(x^e(v), \sigma(e,v)q^e, p_v^e) < \frac{1}{|\alpha^e|},$$

for v incident to e. Any flow values not in $[-|b_0|, |b_0|]$ lead to nonzero circular flows that would cause—due to the strict monotonicity of p^e—a violation of the continuity of pressure, if the pressure values are successively calculated in the flow direction.

We make the same ansatz as in the case of two parallel pipes. The direction of the edges are depicted in Fig. 7. A specific solution of $Aq = b$ is given by $q_s = (-b_0, -b_0, 0, 0, -b_0, 0, -b_0)^T$. Two vectors spanning the kernel of A are

$$q_{K_1} = (0, 1, -1, 1, 0, 0, 0)^T \text{ and } q_{K_2} = (0, 0, 0, 1, -1, 1, 0)^T.$$

This means each solution q of the flow system can be parameterized as

$$q(\lambda_1, \lambda_2) = q_s + \lambda_1 q_{K_1} + \lambda_2 q_{K_2}.$$

To eliminate the second parameter λ_2, we use Lemma 3.7 to compute the flow $q^{e_4}(p_{v_3}(\lambda_1), p_{v_4}(\lambda_1))$, where

$$\begin{aligned} p_{v_3}(\lambda_1) &= p^{e_2}(L^{e_2}, q^{e_2}(\lambda_1, \lambda_2), p_{v_2}(\lambda_1)), \\ p_{v_4}(\lambda_1) &= p^{e_3}(L^{e_3}, q^{e_3}(\lambda_1, \lambda_2), p_{v_2}(\lambda_1)), \\ p_{v_2}(\lambda_1) &= p^{e_1}(L^{e_1}, q^{e_1}(\lambda_1, \lambda_2), p_0). \end{aligned}$$

For $i \in \{1,2,3\}$, the flows $q^{e_i}(\lambda_1, \lambda_2)$ do not depend on λ_2. This means for given λ_1, the parameter λ_2 is determined by

$$\lambda_2(\lambda_1) = q^{e_4}(p_{v_3}(\lambda_1), p_{v_4}(\lambda_1)) - \lambda_1.$$

Note that $p_{v_3}(\lambda_1)$ strictly decreases and $p_{v_4}(\lambda_1)$ strictly increases, which implies that $q^{e_4}(p_{v_3}(\lambda_1), p_{v_4}(\lambda_1))$ and $\lambda_2(\lambda_1)$ are strictly decreasing. The value of λ_1 can be uniquely determined by using the node condition for the pressure in v_5. Like in the case with two parallel pipes, we define

$$\begin{aligned}
p^{\text{red}}(\lambda_1) &= p^{e_5}(L^{e_5}, q^{e_5}(\lambda_1, \lambda_2(\lambda_1)), p_{v_3}(\lambda_1)) \\
&= p^{e_5}(L^{e_5}, -b_0 - \lambda_2(\lambda_1), p_{v_3}(\lambda_1)) \\
p^{\text{blue}}(\lambda_1) &= p^{e_6}(L^{e_6}, q^{e_6}(\lambda_1, \lambda_2(\lambda_1)), p_{v_4}(\lambda_1)) \\
&= p^{e_6}(L^{e_6}, \lambda_2(\lambda_1), p_{v_4}(\lambda_1)) \\
H(\lambda_1) &= p^{\text{red}}(\lambda_1) - p^{\text{blue}}(\lambda_1).
\end{aligned}$$

Because $p_{v_3}(\lambda_1)$ strictly decreases and $\lambda_2(\lambda_1)$ strictly decreases, $p^{\text{red}}(\lambda_1)$ strictly decreases. Because $p_{v_4}(\lambda_1)$ strictly increases and $\lambda_2(\lambda_1)$ strictly decreases, $p^{\text{blue}}(\lambda_1)$ strictly increases. This implies that $H(\lambda_1)$ is strictly decreasing. We look for a $\lambda_1 \in [b_0, 0]$ that satisfies $H(\lambda_1) = 0$.

Let us first consider $\lambda_1 = b_0$. Because of the inequality $p_{v_3}(b_0) > p_{v_4}(b_0)$, we get $q^{e_4}(p_{v_3}(b_0), p_{v_4}(b_0)) > 0$. The relevant flows satisfy

$$\begin{aligned}
q^{e_5}(b_0, \lambda_2(b_0)) &= -b_0 - \lambda_2(b_0) < 0, \\
q^{e_6}(b_0, \lambda_2(b_0)) &= \lambda_2(b_0) > -b_0.
\end{aligned}$$

So, we have

$$\begin{aligned}
p^{\text{red}}(b_0) &= p^{e_5}(L^{e_5}, q^{e_5}(b_0, \lambda_2(b_0)), p_{v_3}(b_0)) \\
&> p^{e_5}(L^{e_5}, 0, p_{v_3}(b_0)) \\
&= p_{v_3}(b_0) > p_{v_4}(b_0)
\end{aligned}$$

and

$$\begin{aligned}
p^{\text{blue}}(b_0) &= p^{e_6}(L^{e_6}, q^{e_6}(b_0, \lambda_2(b_0)), p_{v_4}(b_0)) \\
&< p^{e_6}(L^{e_6}, -b_0, p_{v_4}(b_0)) < p_{v_4}(b_0),
\end{aligned}$$

which implies $H(b_0) > 0$.

Now, the case $\lambda_1 = 0$ is considered. Similar to the first case, $p_{v_3}(0) < p_{v_4}(0)$ implies that $q^{e_4}(p_{v_3}(b_0), p_{v_4}(b_0)) < 0$. The relevant flows satisfy

$$\begin{aligned}
q^{e_5}(0, \lambda_2(0)) &= -b_0 - \lambda_2(0) > -b_0, \\
q^{e_6}(0, \lambda_2(0)) &= \lambda_2(0) < 0.
\end{aligned}$$

This leads to

$$\begin{aligned}
p^{\text{red}}(0) &= p^{e_5}(L^{e_5}, q^{e_5}(0, \lambda_2(0)), p_{v_3}(0)) \\
&< p^{e_5}(L^{e_5}, -b_0, p_{v_3}(0)) < p_{v_3}(0)
\end{aligned}$$

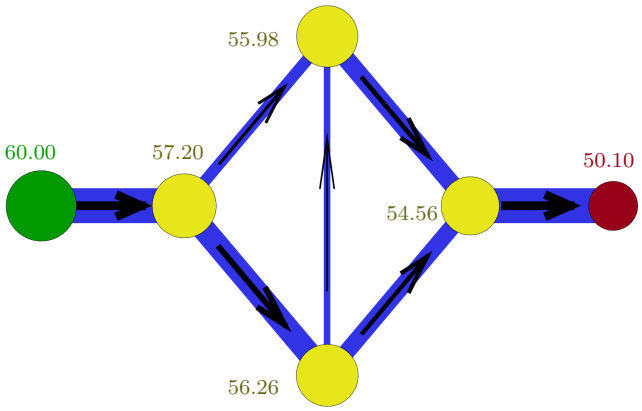

FIG. 8. *Pressure value in* 10^5 Pa *at each node on a diamond graph; source: green, inner node: yellow, sink: red*

and

$$\begin{aligned} p^{\text{blue}}(0) &= p^{e_6}(L^{e_6}, q^{e_6}(0, \lambda_2(0)), p_{v_4}(0)) \\ &> p^{e_6}(L^{e_6}, 0, p_{v_4}(0)) \\ &= p_{v_4}(0) > p_{v_3}(0), \end{aligned}$$

implying $H(0) < 0$. Because $H(\lambda_1)$ strictly decreases and is continuous, Bolzano's intermediate value theorem leads to the existence of a unique $\lambda_1^* \in [b_0, 0]$ with $H(\lambda_1^*) = 0$. The network flow is then determined by $q(\lambda_1^*, \lambda_2(\lambda_1^*))$ and the pressure values are given by

$$p = \left(p_0, p_{v_2}(\lambda_1^*), p_{v_3}(\lambda_1^*), p_{v_4}(\lambda_1^*), p^{\text{red}}(\lambda_1^*), p^{e_7}(L^{e_7}, q^{e_7}(\lambda_1^*, \lambda_2(\lambda_1^*)), p^{\text{red}}(\lambda_1^*))\right)^T.$$

As a numerical example, the pressure values in each node are depicted in Fig. 8 and the flow values on each edge are depicted in Fig. 9. The radius of each node scales with the corresponding pressure value and the thickness of each edge with the corresponding flow value.

4.4. Existence and uniqueness on general networks. The discussion in Sect. 3 provides enough information on the stationary states on the edges to construct stationary states on general graphs that take into account the node conditions (4.2) and (4.3). First, we will look at an important property of the flow system, for which we need the following definition.

DEFINITION 4.2. *Let* $G = (V, E)$ *be a connected graph and let the connected subgraphs* $H = (U, D)$, $I = (W, F)$ *of* G *be disjoint. Then the set of edges* $S \subset E$ *is called a* separator *for the subgraphs* H *and* I*, if the removal of* S *from the edges* E *of* G *separates* G *into the distinct connected parts* H *and* I*.*

The Lemma consist of two parts. On the one hand, it is a rigorous formulation of the conservation of mass on each part of the network. On the other hand, it allows us to construct admissible flows on subgraphs $H = (U, D), I = (W, F)$ of G, if we already have a admissible flow on H. We use nodes v and edges e to index to component of vectors. For $b \in \mathbb{R}^{|V|}$, the expression b_v refers to the component corresponding to v.

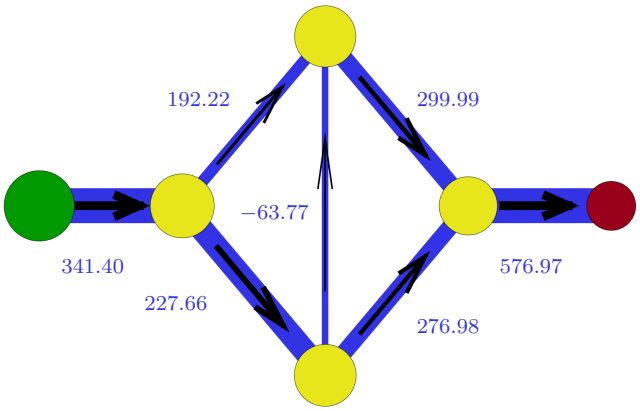

FIG. 9. *Flow value in* $\mathrm{kg\,m^{-2}\,s^{-1}}$ *at each edge on a diamond graph; in- and outflows do not sum to zero, because the pipes have different diameter (s. Sec. 7)*

The vector $\mathbf{1}$ is the vector of only ones in the appropriate space, which will be clear in the context.

LEMMA 4.3. *Let* $G = (V, E)$ *be a connected graph,* $H = (U, D), I = (W, F)$ *disjoint connected subgraphs of* G *and* S *a separator for* H *and* I*. Every edge* $e \in S$ *has two incident vertices* $u_e \in U$ *and* $w_e \in W$*. We denote the incidence matrix of* G *by* $A \in \mathbb{R}^{|V|\times|E|}$*, where* $A_{ij} = \sigma(v_i, e_j) \in \{-1, 0, 1\}$ *and the linear subspace of admissible node outflows*

$$B = \left\{ b \in \mathbb{R}^{|V|} : \mathbf{1}^T b = 0 \right\}.$$

Let $b \in B$ *and let* $q \in \mathbb{R}^{|E|}$ *be a solution of*

$$A\,q = b.$$

We set $a_v := b_v$ *for all* $v \in U$ *that are not incident to an edge in* S *and* $c_v := b_v$ *for all* $v \in W$*, that are not incident to an edge in* S*. For the other edges* $e \in S$*, we set*

$$\begin{aligned} a_{u_e} &:= b_{u_e} - \sum_{s\in S\cap E_0(u_e)} \sigma(s, u_e)\, q^s, \\ c_{w_e} &:= b_{w_e} - \sum_{s\in S\cap E_0(w_e)} \sigma(s, w_e)\, q^s, \end{aligned} \tag{4.4}$$

where $E_0(u_e)$ *(*$E_0(w_e)$*) denotes the set of edges incident to* u_e *(*w_e*).*

Then these new defined outflow vectors sum to zero, i.e.,

$$\sum_{u\in U} a_u = \sum_{w\in W} c_w = 0. \tag{4.5}$$

Furthermore, for

$$q^D := \left(q^d\right)_{d\in D},\ q^F := \left(q^f\right)_{f\in F}$$

and with the incidence matrix for the graph (V, D) denoted by A^H and for (V, F) by A^I, we have

$$A^H q^D = \begin{pmatrix} a \\ 0_{|W|} \end{pmatrix}, \quad A^I q^F = \begin{pmatrix} 0_{|U|} \\ c \end{pmatrix}. \tag{4.6}$$

Hence, the restrictions q^D and q^F are solutions of the flow system on the subgraphs H and I for the naturally defined outflow vectors a and c.

Proof. We know that $E = D \cup S \cup F$ and the sets D, S, F are pairwise disjoint. Without loss of generality, we assume that the edges E are ordered in such a way that the adjacency matrix A can be written as $[A^H A^S A^I]$, where A^S is the incidence matrix of (V, S). Analogously, the vector q can be written as

$$q^T = \left[\left(q^D\right)^T \left(q^S\right)^T \left(q^F\right)^T \right].$$

Furthermore, let us also assume that the vertices are in order such that

$$b^T = \left[\left(b^U\right)^T \left(b^W\right)^T \right], \text{where } b^U := \begin{pmatrix} b_u \end{pmatrix}_{u \in U}, \; b^W := \begin{pmatrix} b_w \end{pmatrix}_{w \in W}.$$

Then the linear system of equations can be written as

$$\left[A^H A^S A^I\right] \begin{bmatrix} q^D \\ q^S \\ q^F \end{bmatrix} = \begin{bmatrix} b^U \\ b^W \end{bmatrix}. \tag{4.7}$$

The equation

$$\begin{bmatrix} b^U \\ b^W \end{bmatrix} - A^S q^S = \begin{bmatrix} a \\ c \end{bmatrix}$$

is equivalent to (4.4). We can write (4.7) as

$$A^H q^D + A^H q^F = \begin{bmatrix} a \\ c \end{bmatrix}.$$

Since no edge in D is connected to a node in W and no edge in F is connected to a node in U, we have $\left(A^H q^D\right)_w = 0$ for all $w \in W$ and $\left(A^I q^F\right)_u = 0$ for all $u \in U$. Thus, (4.6) holds and only (4.5) remains to be shown. First, we use the fact that for each edge $e \in S$,

$$a_{u_e} + c_{w_e} = b_{u_e} + b_{w_e}$$

holds. This shows that

$$\sum_{u \in U} a_u + \sum_{w \in W} c_w = \sum_{v \in V} b_v = 0. \tag{4.8}$$

Let us assume that $\sum_{u \in U} a_u \neq 0$. Then,

$$a \notin \operatorname{span}\left(\left\{\mathbf{1}_{|U|}\right\}\right)^\perp = \ker\left(\left(A^H\right)^T\right)^\perp = \operatorname{im}(A^H).$$

This means the system $A^H \tilde{q}^D = a$ is not solvable, which is a contradiction to $A^H q^D = a$. Hereby, we have that $\sum_{u \in U} a_u = 0$, and $\sum_{w \in W} b_w = 0$ follows from (4.8). ∎

EXAMPLE 1. *In the case of two parallel pipes with all edges pointing from left to right (see Fig. 6), a solution of* $Aq = (b_0, 0, 0, -b_0)^T$ *is* $q = (-b_0, -0.5b_0, -0.5b_0, -b_0)^T$. *Note that this solution does not have to satisfy the pressure continuity condition in general, but it would, if the two parallel pipes were identical. Let us define the separator* $S = \{e_2, e_3\}$ *as the set of the two middle edges. The two new subgraphs* $H = \big(\{v_0, v_1\}, \{e_1\}\big), I = \big(\{v_2, v_3\}, \{e_4\}\big)$ *correspond to the left and right pipe, respectively. The new node outflows as described in* (4.4) *are defined as*

$$\begin{aligned} a_{v_0} &:= b_{v_0} = b_0, & c_{v_2} &= b_{v_2} - q^{e_2} - q^{e_3} = b_0, \\ a_{v_1} &:= b_{v_1} + q^{e_2} + q^{e_3} = -b_0, & c_{v_3} &= b_{v_3} = -b_0. \end{aligned}$$

With

$$A^H := \begin{pmatrix} -1 \\ +1 \\ 0 \\ 0 \end{pmatrix}, \qquad A^I := \begin{pmatrix} 0 \\ 0 \\ -1 \\ +1 \end{pmatrix},$$

it is easy to see that the solution q *satisfies*

$$A^H q^{e_1} = \begin{pmatrix} a_{v_0} \\ a_{v_1} \\ 0 \\ 0 \end{pmatrix} \qquad A^I q^{e_4} = \begin{pmatrix} 0 \\ 0 \\ c_{v_2} \\ c_{v_3} \end{pmatrix}.$$

Lemma 4.3 yields the following useful implication concerning the monotonicity of the admissible flows with regard to the node outflows.

COROLLARY 4.4. *Let a connected graph* $G = (V, E)$ *with incidence matrix* A *be given. Let* t, u *and* w *be three distinct boundary nodes of* G. *Consider the linear system* $Aq = b$. *For a given* $\tilde{b}_u$, *the vector* $\tilde{b}$ *has entries equal to* b *except in the nodes* u *and* t, *where its values are* $\tilde{b}_u$ *and* $\tilde{b}_t := \tilde{b}_u - \sum_{v \in V \setminus \{u,t\}} b_v$.

For each $\tilde{b}_u > b_u$ *and a specific solution* $\tilde{q}$ *of* $A\tilde{q} = \tilde{b}$, *there exists a path between* u *and* w *such that for all edges on the path the flows fulfill*

$$\sigma(e, u_e)\, \tilde{q}^e \geq \sigma(e, u_e)\, q^e,$$

where u_e *is the node incident to* e *that is closer to* u.

Proof. Assume the contrary. This means there exists a boundary flow $\tilde{b}_u > b_u$ and a separator S that separates G into $H = (U, D)$ and $I = (W, F)$ with $u \in U$ and $w \in W$, such that for all $e \in S$ the inequality

$$\sigma(e, u_e)\, \tilde{q}^e < \sigma(e, u_e)\, q^e$$

holds true, if $\tilde{q}$ is a solution of $A\tilde{q} = \tilde{b}$, where $\tilde{b}$ is identical to b except in u and t. For both the system $Aq = b$ and $A\tilde{q} = \tilde{b}$, one can apply Lemma 4.3. We denote the set of all nodes incident to a edge $e \in S$ by

$$T := \{v \in V \mid \sigma(e, v) \neq 0 \text{ for one } e \in S\}.$$

Without loss of generality, we assume $u \notin T$ (since u is a boundary node, it is incident to only one edge—one can divide the edge into two by inserting an artificial node without changing the flows). Define

$$a_v := \begin{cases} b_v, & v \in U \setminus T, \\ b_v - \sum_{s \in S \cap E_0(v)} \sigma(s,v) q^s, & v \in U \cap T, \end{cases}$$
$$\tilde{a}_v := \begin{cases} \tilde{b}_v, & v \in U \setminus T, \\ \tilde{b}_v - \sum_{s \in S \cap E_0(v)} \sigma(s,v) \tilde{q}^s, & v \in U \cap T. \end{cases}$$

There are two cases to consider: First, $t \notin U$ and second, $t \in U$. In the first case, we get

$$\begin{aligned} 0 &= b_u + \sum_{v \in U \setminus \{u\}} a_v \\ &= b_u + \sum_{\substack{v \in U \setminus T, \\ v \neq u}} a_v + \sum_{\substack{v \in U \cap T: \\ v \neq u}} \left[b_v - \sum_{s \in S \cap E_0(v)} \sigma(s,v) q^s \right] \\ &< \tilde{b}_u + \sum_{\substack{v \in U \setminus T, \\ v \neq u}} \tilde{a}_v + \sum_{\substack{v \in U \cap T: \\ v \neq u}} \left[\tilde{b}_v - \sum_{s \in S \cap E_0(v)} \sigma(s,v) \tilde{q}^s \right] \end{aligned}$$

(because $\tilde{b}_u > b_u$ and $\sigma(s,v)\tilde{q}^s < \sigma(s,v) q^s$ by assumption, while for the other terms equality holds per definition)

$$= \sum_{v \in U} \tilde{a}_v = 0.$$

In the second case,

$$\begin{aligned} 0 &= b_u + \sum_{v \in U \setminus \{u\}} a_v \\ &= b_u + b_t + \sum_{\substack{v \in U \setminus T, \\ v \notin \{u,t\}}} a_v + \sum_{\substack{v \in U \cap T, \\ v \notin \{u,t\}}} \left[b_v - \sum_{s \in S \cap E_0(v)} \sigma(s,v) q^s \right] \\ &< - \sum_{v \in U \setminus \{u,t\}} b_v + \sum_{\substack{v \in U \setminus T, \\ v \notin \{u,t\}}} \tilde{a}_v + \sum_{\substack{v \in U \cap T, \\ v \notin \{u,t\}}} \left[\tilde{b}_v - \sum_{s \in S \cap E_0(v)} \sigma(s,v) \tilde{q}^s \right] \end{aligned}$$

(because $\sigma(s,v)\tilde{q}^s < \sigma(s,v) q^s$ by assumption, while for the other terms equality holds per definition)

$$= \tilde{b}_u + \tilde{b}_t + \sum_{v \in U \setminus \{u,t\}} \tilde{a}_v = 0.$$

So in both cases, we get a contradiction. This means the assumption was wrong and there exists a path between u and w such that the flow values fulfill

$$\sigma(e, u_e)\, \tilde{q}^e \geq \sigma(e, u_e)\, q^e$$

along this path. □

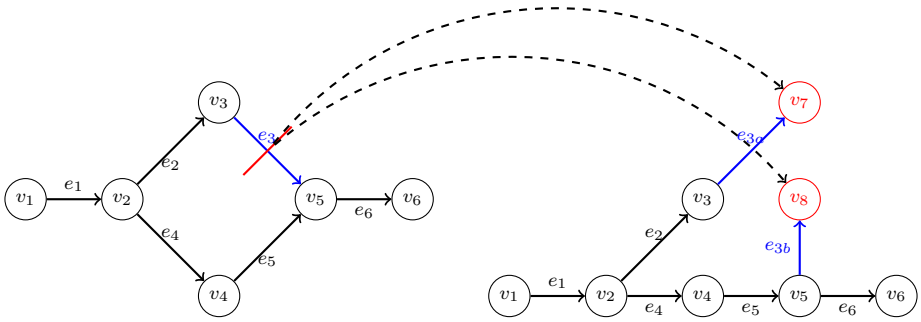

FIG. 10. *Cutting an inner edge in a graph with one circle results in a tree shaped graph*

For the construction, the monotonicity properties of the stationary states on the edges are essential. If for a fixed value of q^e, the value of the pressure p^e is strictly increased at one of the ends of the pipe that corresponds to the edge $e \in E$, that is at 0 or L^e, also the pressure at the other end of the pipe (that is L^e or 0, respectively) will strictly increase.

If for a fixed pressure value p_0^e at the end 0 of the pipe that corresponds to the edge $e \in E$, the flow rate q^e is increased, then the pressure value $p^e(L^e, q^e, p_0^e)$ at the other end of the pipe is decreased.

If for a fixed pressure value $p_{L^e}^e$ at the end L^e of the pipe that corresponds to the edge $e \in E$, the flow rate q^e is increased, then the pressure value $p^e(0, -q^e, p_L^e)$ at the other end of the pipe is also increased.

The idea of the proof for general networks is to inductively reduce the number of circles in the graph by cutting one edge in the middle in half. The solution on a graph with no circles—that is a tree—was already discussed in Lemma 4.1. The idea is illustrated in Figs. 10 and 11. For a node v we will denote the set of ingoing edges by

$$E_+(v) := \{e \in E \,|\, \sigma(e, v) = 1\}$$

and as in the beginning of Sect. 4 let

$$E_0(v) := \{e \in E \mid \sigma(e, v) \neq 0\}.$$

The following theorem states that sufficiently small boundary flows determine unique stationary flow in the network. In particular, the pressure values in the nodes and the flow values on the edges are uniquely determined. This solution fulfills the Kirchhoff flow condition and the continuity of pressure, i.e., no matter from which ingoing edge to a node we calculate the pressure function, we always arrive at the same value in this node. We also take care of the restricted domain of the pressure functions p^e. If our boundary flows are small enough, the one given boundary pressure fulfills the subsonic flow condition and the compressibility factor is positive, then—thanks to the continuity of our pressure functions—these properties are preserved in all other nodes.

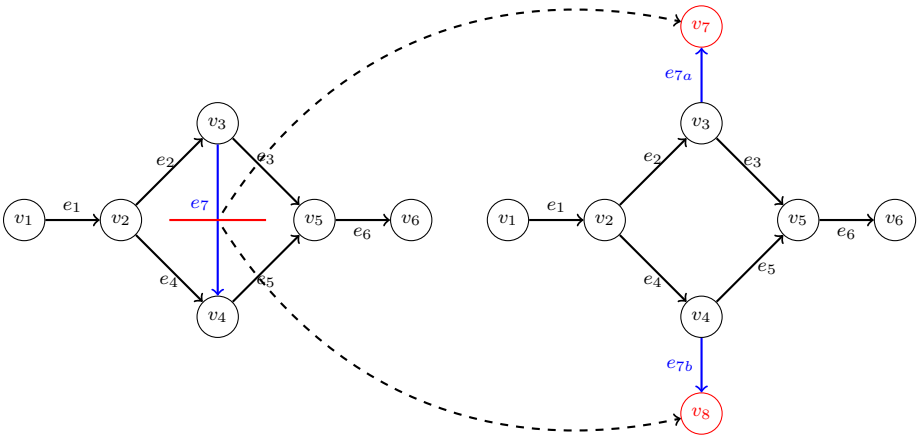

FIG. 11. *Cutting an inner edge in a graph with two circles results in a graph with one circle*

THEOREM 4.5. *Let a finite connected directed graph $G = (V, E)$ be given. The directed incidence matrix of G is denoted by A with $A_{ij} = \sigma(e_j, v_i)$ (see (4.1)). Each edge $e \in E$ of the graph corresponds to an interval $[0, L^e]$. Define the space of admissible outflows*

$$B := \left\{ b \in \mathbb{R}^{|V|} : \sum_{v \in V} b_v = 0 \right\}.$$

In one boundary node v_0, a pressure $p_0 \in \left(|b_{v_0}| \sqrt{RT^e}, \frac{1}{|\alpha^e|} \right), e \in E_0(v_0)$ is given.

There is a constant $C(p_0, G) > 0$ that only depends on p_0 and G—including the properties of each edge—such that for every $b \in B$ with sufficiently small norm in the sense that

$$\|b\| < C(p_0, G)$$

there exists a unique subsonic stationary state $(p, q) \in \mathbb{R}^{|V|} \times \mathbb{R}^{|E|}$, that satisfies

$$A\, q = b$$

and for $v \in V$, for all $e = (u, v) \in E_+(v)$, we have

$$p_v = p^e(x(v), q^e, p_u).$$

REMARK 4. *In this remark, we explain how our proof shows the uniqueness of the solution. The initial step of the proof by induction starts with a tree. On a tree graph, for given boundary flows, the linear system for the flow rates has a unique solution, which means that one can calculate all pressure values starting from the root node. The induction assumption then requires to have a unique solution on a graph with* $\dim(\ker(A)) \leq n$, *if the boundary flows are known. A graph with* $\dim(\ker(A)) = n+1$ *can, by cutting one edge, be interpreted as a graph with* $\dim(\ker(A)) \leq n$ *with one unknown flow value λ through the cut edge. If one knew the value λ the resulting state*

would be unique due to the induction assumption. This is because after removing all fundamental circles in the graph by the described technique, the resulting graph is a tree. However, in order to fulfill the continuity of pressure condition, the parameter λ has to be a root of the auxiliary function H, which is given by the difference of the pressure values in the artificial boundary nodes that were generated by cutting an edge in a fundamental circle. We show that this root of H is unique. This means every flow value in the network is uniquely determined, which allows the calculation of all pressure values via the functions p^e along each edge starting from the node, where p_0 is prescribed. In this way, our proof shows the uniqueness of stationary states on networks for given boundary data. The uniqueness is of course only possible by postulating the continuity of pressure condition.

The choice, which edge to cut, can be seen as choosing a basis for the kernel of A, because each fundamental circle corresponds to a basis vector of the kernel of A. If one retains a unique flow vector in one basis, a change of the basis only changes the representation of q, but not its value. The resulting stationary state is therefore independent of the choice of which edges to cut.

Proof. [Theorem 4.5] The proof of the theorem is based on mathematical induction over $\dim(\ker(A))$.

Initial step.
We start with the case of a tree that is $\dim(\ker(A)) = 0$. Lemma 4.1 gives the unique solvability for small flows q^e. Since $Aq = b$ has a unique solution, we can write $q = A^+ b$ with the pseudo inverse A^+ of A. This means $\|q\|_\infty \leq \|A^+\|_\infty \|b\|_\infty$. Because each function p^e is continuous in q^e, we can conclude that there is a $C(p_0, G) > 0$, such that every q^e satisfies the assumptions of Lemma 4.1 for an outflow vector satisfying $\|b\| \leq C(p_0, G)$. Now, we want to show that each pressure in a boundary node $v_\partial \neq v_0$ decreases as a function of $\sigma(e, v_\partial) q^e$, for $e \in E_0(v_\partial)$, if the pressure in v_0 is fixed and all flow rates except in the edges incident to v_0 and v_∂ are fixed as well. The path $P = (V^P, E^P)$ between v_∂ and v_0 is the only part of the tree, where the flow values can change. Every other edge in the graph is part of a subtree with only one vertex—the root of the subtree—in V^P. On the subtree, every node outflow is determined except the one in its root. Hence, the flow system on the subtree has a unique solution only depending on the fixed boundary flows. Since the flow value on each edge $e \notin E^P$ is determined, we can redefine the node outflows for vertices on the path to reduce the linear system:

$$b_v^P := b_v - \sum_{e \in E_0(v) \setminus E^P} \sigma(e, v) q^e, \quad v \in V^P.$$

Then, for the subgraph of the path, we retain $A^P q^P = b^P$, with

$$A^P := \begin{pmatrix} \sigma(e_1^P, v_1^P) & \cdots & \cdots & 0 \\ \sigma(e_1^P, v_2^P) & \sigma(e_2^P, v_2^P) & 0 & \vdots \\ 0 & \sigma(e_2^P, v_3^P) & \ddots & \vdots \\ \vdots & \vdots & \ddots \quad \ddots & 0 \\ \vdots & \vdots & \sigma(e_{m-1}^P, v_{k-1}^P) & \sigma(e_m^P, v_{k-1}^P) \\ 0 & 0 & 0 & \sigma(e_m^P, v_k^P) \end{pmatrix}.$$

Here, we have used the notation

$$v_1^P := v_\partial, \quad v_k^P := v_0, \quad V^P := \{v_1^P, \dots, v_k^P\}, \quad E^P := \{e_1^P, \dots, e_m^P\}.$$

Using forward substitution, one can see that the diagonal elements of A^P fulfill

$$\sigma(e_j^P, v_j^P) q_j^P = \sum_{i=1}^{j} b_i^P.$$

Every flow $\sigma(e_j^P, v_j^P) q_j^P$ linearly increases as a function of $\sigma(e, v_\partial) q^e = b_1^P$, $e \in E_0(v_\partial)$. This means—due to the monotonicity on one pipe—that for an increasing flow $\sigma(e, v_\partial) q^e$, the pressure values decrease.

On the path P, this can be seen by starting from v_0 and calculating the pressure along each edge. On the first edge, the pressure $p^{e_1^P}(L^{e_1^P}, \sigma(e_1^P, v_0) q^{e_1^P}, p_0)$ decreases if the flow increases. Now on every further edge, the pressure is a function of the ingoing pressure—which is decreasing—and the flow—which is increasing—meaning the pressure is a decreasing function with respect to the flow $\sigma(e, v_\partial) q^e, e \in E_0(v_\partial)$. For the pressure values in nodes that are not in V^P, the situation is even easier. We have already stated that each node in $V \setminus V^P$ is part of a subtree with root in V^P. The pressure value in the root decreases as a function of $\sigma(e, v_\partial) q^e, e \in E_0(v_\partial)$. The flow values on the edges of the subtree are constant; hence the pressure value in each node decreases regarding $\sigma(e, v_\partial) q^e, e \in E_0(v_\partial)$.

Induction assumption.
Let $\dim(\ker(A)) \leq n$. Then for each $b \in B$ with $\|b\| \leq C(p_0, G)$, there exists a unique solution (p, q) satisfying the Kirchhoff conditions for the flow and the node coupling conditions for the pressure. Moreover, for each boundary node $v \neq v_\partial$ the values p_v strictly decrease as a function of b_v, if the values of all other boundary flow rates—except in v_∂—are fixed.

Induction step.
Assume that the dimension of $\ker(A)$ is $n+1$. We consider the new graph G^c that is generated by cutting one of the edges of the given graph G in the middle. By the cut, we generate a new graph with two additional boundary nodes. To choose the edge that we cut, we consider a basis of $\ker(A)$. We choose an edge e_c for which a vector $q_{\ker}$ that is contained in the basis has a nonzero entry. Let A^c denote the incidence matrix for $G^c = (V^c, E^c)$. The basis vectors of $\ker(A)$ with zero entries at the edge e_c can be easily transformed into basis vectors of $\ker(A^c)$ by setting the components zero for both new edges. However, for the chosen basis vector $q_{\ker}$, this is not possible. Moreover, the cut does not generate new circles. Thus, the dimension of $\ker(A^c)$ is n at most. Therefore, we can apply our induction assumption to construct a stationary flow on G^c for the prescribed boundary data. There exists a unique stationary flow on G^c for the prescribed boundary data p_0 and b^c if $\|b^c\| < C(p_0, G^c)$ for a certain constant $C(p_0, G^c) > 0$. The values in b^c are given by those of b for nodes that were in the old graph. The outflows in the two new nodes v_{red} and v_{blue} generated by the cut are $b_{v_{\text{red}}} = \lambda$ and $b_{v_{\text{blue}}} = -\lambda$ for $\lambda \in \mathbb{R}$. It is clear that $\sum_{v \in V^c} b_v^c = 0$ holds. To make the dependence more apparent, the new outflow vector will be denoted as b_λ^c. The additional constraint $b_{v_{\text{red}}} = -b_{v_{\text{blue}}}$ refers to the conservation of mass through the cut. Due to our induction assumption, for sufficiently small λ, there exists a unique stationary state $(p_\lambda^c, q_\lambda^c)$ satisfying $A^c q_\lambda^c = b_\lambda^c$ and the continuity of pressure on G^c.

Let us define

$$p^{\text{red}}(\lambda) := p^{e_{\text{red}}}(\tfrac{1}{2}L^{e_c}, \lambda, p_{u_{\text{red}}}),$$
$$p^{\text{blue}}(\lambda) := p^{e_{\text{blue}}}(\tfrac{1}{2}L^{e_c}, -\lambda, p_{u_{\text{blue}}}),$$

where e_{red} and e_{blue} are the new edges with length $\frac{1}{2}L^{e_c}$ generated by the cut, which are incident to v_{red} and v_{blue}, respectively, u_{red} is adjacent to v_{red}, and u_{blue} is adjacent to v_{blue}. We also define the auxiliary function

$$H(\lambda) := p^{\text{red}}(\lambda) - p^{\text{blue}}(\lambda).$$

The induction assumption states that p^{red} strictly decreases and p^{blue} strictly increases with respect to λ. It follows that H strictly decreases. Now, we show the existence of a λ with $H(\lambda) > 0$ and a λ with $H(\lambda) < 0$. First, we show that for large λ, there exists a path $P = (V^P, E^P)$ between v_{red} and v_{blue}, such that the flow is directed from v_{blue} to v_{red} on the path. For convenience and readability, we drop the index λ, if we refer to components of a vector. We choose

$$\lambda_- := \sum_{v \in V \setminus \{v_{\text{red}}, v_{\text{blue}}\}} |b_v|.$$

Note that if $C(p_0, G^c) > 0$ is chosen sufficiently small, the state $(p_{\lambda_-}, q^c_{\lambda_-})$ stays subsonic and $p_v < \frac{1}{|\alpha^e|}$, $e \in E_0(v)$ holds for all $v \in V$. Let us suppose that a path with the flow directed from v_{blue} to v_{red} does not exist. Then there exists a separator S that splits the graph G^c into the two disjoint subgraphs $G^{\text{red}} := (V^{\text{red}}, E^{\text{red}})$ and $G^{\text{blue}} := (V^{\text{blue}}, E^{\text{blue}})$ with $v_{\text{red}} \in V^{\text{red}}, v_{\text{blue}} \in V^{\text{blue}}$, such that the flow direction is directed from V^{red} to V^{blue}. Each edge $e \in S$ has two incident nodes $v_e^{\text{red}} \in V^{\text{red}}$ and $v_e^{\text{blue}} \in V^{\text{blue}}$. Formally, the flow direction on the separator can be expressed as $\sigma(e, v_e^{\text{red}}) q^e_{\lambda_-} < 0$ for all $e \in S$ (keep in mind that for edges directed from v_e^{red} to v_e^{blue}, $\sigma(e, v_e^{\text{red}}) = -1$ holds). Now, Lemma 4.3 is applicable. We define $b_v^{\text{red}} := b_v^c$ for all $v \in V^c$ that are not incident to an edge in S and for all $e \in S$ we set

$$b^{\text{red}}_{v_e^{\text{red}}} := b^c_{v_e^{\text{red}}} - \sum_{s \in S \cap E_0(v_e^{\text{red}})} \sigma(s, v_e^{\text{red}}) q^s_{\lambda_-}.$$

The vector b^{red} is the right side of the flow system $A^{\text{red}} q^{\text{red}}_{\lambda_-} = b^{\text{red}}$ on G^{red} and more importantly $\sum_{v \in V^{\text{red}}} b_v^{\text{red}} = 0$ holds. Let us denote (like in Corollary 4.4)

$$T := \{v \in V \mid \sigma(e, v) \neq 0 \text{ for one } e \in S\}.$$

This leads to

$$\begin{aligned} 0 = \sum_{v \in V^{\text{red}}} b_v^{\text{red}} &= \lambda_- + \sum_{\substack{v \in V^{\text{red}} \setminus T, \\ v \neq v^{\text{red}}}} b_v^{\text{red}} + \sum_{\substack{v \in V^{\text{red}} \cap T, \\ v \neq v^{\text{red}}}} b_v^{\text{red}} \\ &> \lambda_- + \sum_{\substack{v \in V^{\text{red}} \setminus T, \\ v \neq v^{\text{red}}}} b_v^{\text{red}} + \sum_{\substack{v \in V^{\text{red}} \cap T, \\ v \neq v^{\text{red}}}} b_v^c \end{aligned}$$

(because $\sigma(e, v_e^{\text{red}}) q^e_{\lambda_-} < 0$ and thus $b^{\text{red}}_{v_e^{\text{red}}} > b^c_{v_e^{\text{red}}}$)

$$= \sum_{v \in V \setminus \{v_{\text{red}}, v_{\text{blue}}\}} |b_v^c| + \sum_{v \in V^{\text{red}} \setminus \{v_{\text{red}}\}} b_v^c \geq 0,$$

which is a contradiction. Hence, a path with flow direction from v^{blue} to v^{red} has to exist. Because the pressure decreases along the path, if we have only one flow direction, $H(\lambda_-) < 0$ follows. The argument applies analogously for the direction from v^{red} to v^{blue}, but one has to pay attention to the negative sign in $b^c_{v_{\text{red}}} = -\lambda$. There exists a flow $\lambda_+ < 0$ fulfilling $H(\lambda_+) > 0$. Because H is continuous and decreasing, Bolzano's intermediate value theorem implies that there exists a unique number $\lambda^* \in (\lambda_+, \lambda_-)$ satisfying $H(\lambda^*) = 0$. Hence, there exists a unique solution $(p^c_{\lambda^*}, q^c_{\lambda^*})$ on the cut graph. Hereby, a solution on the original graph G can be constructed by setting all pressure values p_v to their corresponding values p^c_v and dropping the values in v_{red} and v_{blue}. The flow values can be retained by setting the $q^e = q^c_e$ for all edges except e_c, which is assigned the value $\sigma(e_{\text{red}}, v_{\text{red}})\lambda^*$. It only remains to be shown that the pressure in a boundary node v decreases as a function of b_v, if the values of all other boundary flow rates except in another boundary node v_∂ are fixed. Corollary 4.4 states the existence of a path between v and v_0, where the pressure p_0 is given, with increasing flow with respect to b_v. The pressure on each edge decreases with respect to the flow and increases with respect to the pressure in the left node. We can write the pressure in v as a composition of the pressure functions along the path to v_0. On the path, the flow values increase with respect to b_v, meaning consecutively—starting from p_0—the node pressures decrease with respect to b_v. Hence, the pressure in p_v decreases as a function of b_v (it *strictly* decreases because of the strict decrease one has on the boundary edge incident to v) and the induction assumption for the graph has been shown. Note that the path of increasing flows does not have to be independent of the outflows to ensure the stated monotonicity properties of the pressure. Thus, our proof by induction is complete. ∎

REMARK 5. *The proof does not require the explicit representation of the pressure solution. Indeed, only its monotonicity properties are decisive, which makes the argumentation applicable to similar models such as the Weymouth equation. Furthermore, if a subset of the edges represents a compressor modeled by a function $f^e(p_u, q)$ with the outgoing pressure given by $p_v = f^e(p_u, q), e = (u, v)$ and this function has the same monotonicity properties as p^e, then a similar proof is applicable and we can show the existence of a unique solution for gas networks with compressors. The monotonicity properties for f^e are reasonable, because a higher ingoing pressure will result in a higher outgoing pressure and an increased flow will result in a smaller compression ratio (for details see [Koch et al., 2015, Chapter 2]).*

5. Conclusion.

We have shown the existence of unique stationary states for networks for the transportation of real gas for given suitable boundary data. Our result holds for arbitrary finite graphs. The proof is based on the monotonicity properties of the solution with respect to the boundary data. In the future, we plan to extend the analysis to include also control elements (e.g. compressors) in the graph. Moreover, sometimes the inclusion of thermal effects in the analysis is desirable; see [Keenan, 1995].

6. Acknowledgements.

We would like to thank the reviewers for their helpful constructive comments. This work was supported by DFG in the framework of the Collaborative Research Centre CRC/Transregio 154, Mathematical Modelling, Simulation and Optimization Using the Example of Gas Networks, project C03, B05 and A05.

REFERENCES

[Bakhvalov, 1970] Bakhvalov, N. S. (1970). The existence in the large of a regular solution of a quasilinear hyperbolic system. *Z. Vycisl. Mat. i Mat. Fiz. 10*, pages 969–980.

[Banda et al., 2006] Banda, M. K., Herty, M., and Klar, A. (2006). Coupling conditions for gas networks governed by the isothermal Euler equations. *NHM*, 1(2):295–314.

[Bressan et al., 2014] Bressan, A., Canic, S., Garavello, M., Herty, M., and Piccoli, B. (2014). Flows on networks: recent results and perspectives. *EMS Surveys in Mathematical Sciences*, 1(1):47–111.

[Bressan et al., 2015] Bressan, A., Chen, G., Zhang, Q., and Zhu, S. (2015). No BV bounds for approximate solutions to p-system with general pressure law. *Journal of Hyperbolic Differential Equations*, 12(04):799–816.

[Cerbe, 2008] Cerbe, G. (2008). *Grundlagen der Gastechnik: Gasbeschaffung - Gasverteilung - Gasverwendung*. Hanser.

[Colombo et al., 2009] Colombo, R. M., Guerra, G., Herty, M., and Schleper, V. (2009). Optimal control in networks of pipes and canals. *SIAM J. Control and Optimization*, 48(3):2032–2050.

[Colombo and Marcellini, 2010] Colombo, R. M. and Marcellini, F. (2010). Smooth and discontinuous junctions in the p-system. *Journal of Mathematical Analysis and Applications 361*, pages 440–456.

[de Almeida et al., 2014] de Almeida, J. C., Velásquez, J., and Barbieri, R. (2014). A methodology for calculating the natural gas compressibility factor for a distribution network. *Petroleum Science and Technology*, 32(21):2616–2624.

[Garavello, 2009] Garavello, Mauro, P. B. (2009). Conservation laws on complex networks. *Annales de l'I.H.P. Analyse non linaire*, 26(5):1925–1951.

[Ghanbari et al., 2011] Ghanbari, A., Fred, F. F., and Rieke, H. (2011). Newly developed friction factor correlation for pipe flow and flow assurance. *Journal of Chemical Engineering and Materials Science*, 2(6):83–86.

[Gugat et al., 2015] Gugat, M., Hante, F. M., Hirsch-Dick, M., and Leugering, G. (2015). Stationary states in gas networks. *NHM*, 10(2):295–320.

[Gugat and Herty, 2011] Gugat, M. and Herty, M. (2011). Existence of classical solutions and feedback stabilization for the flow in gas networks. *ESAIM: Control, Optimisation and Calculus of Variations*, 17(1):28–51.

[Gugat et al., 2012] Gugat, M., Herty, M., Klar, A., Leugering, G., and Schleper, V. (2012). Well-posedness of networked hyperbolic systems of balance laws. In *Constrained optimization and optimal control for partial differential equations*, volume 160 of *Internat. Ser. Numer. Math.*, pages 123–146. Birkhäuser/Springer Basel AG, Basel.

[Keenan, 1995] Keenan, P. T. (1995). Thermal simulation of pipeline flow. 32(4):1225–1262.

[Koch et al., 2015] Koch, T., Hiller, B., Pfetsch, M. E., and Schewe, L. (2015). *Evaluating gas network capacities*, volume 21. SIAM.

[Martin et al., 2006] Martin, A., Möller, M., and Moritz, S. (2006). Mixed integer models for the stationary case of gas network optimization. *Mathematical Programming B*, 105:563 – 582.

[Reigstad, 2014] Reigstad, G. A. (2014). Numerical network models and entropy principles for isothermal junction flow. *Networks and Heterogeneous Media*, 9(1):65–95.

[Ríos-Mercado et al., 2002] Ríos-Mercado, R. Z., Wu, S., Scott, L. R., and Boyd, E. A. (2002). A reduction technique for natural gas transmission network optimization problems. *Annals OR*, 117(1-4):217–234.

[Schmidt et al., 2014] Schmidt, M., Steinbach, M. C., and Willert, B. M. (2014). High detail stationary optimization models for gas networks - part 2: Validation and results. Technical report, Friedrich-Alexander-Universität Erlangen-Nürnberg, Department Mathematik; Leibniz Universität Hannover, Institut für Angewandte Mathematik.

[Schroeder Jr et al., 2010] Schroeder Jr, D. W. et al. (2010). A tutorial on pipe flow equations. In *PSIG Annual Meeting*. Pipeline Simulation Interest Group.

[Zou et al., 2005] Zou, G., Cheraghi, N., and Taheri, F. (2005). Fluid-induced vibration of composite natural gas pipelines. *International Journal of Solids and Structures*, 42(34):1253 – 1268.

7. Appendix. For the convenience of the reader Tables 1–7 below contain the data used in the numerical examples presented in Figs. 8 and 9. The constant α^e in the compressibility factor model is computed via (see e.g., [Schmidt et al., 2014])

$$\alpha^e = \frac{0.257}{p_c} - 0.533\frac{T_c}{p_c T^e}.$$

We have used the formula of Chen (s. [Cerbe, 2008]), which is an explicit estimate for the Colebrook–White law, to calculate realistic values for $\theta^e = \frac{\lambda^e_{\text{fric}}}{D^e}$. The equations for the Reynolds number and the friction factor read as follows:

$$Re^e := \frac{q^e D^e}{\eta_v},$$
$$\frac{1}{\sqrt{\lambda^e_{\text{fric}}}} = -2\log_{10}\left(\frac{\frac{k^e}{D^e}}{3.7065} - \frac{5.0425}{Re^e}\log_{10}\left[\frac{\left(\frac{k^e}{D^e}\right)^{1.1098}}{2.8257} + \frac{5.8506}{(Re^e)^{0.8981}}\right]\right).$$

Since for the stationary states q^e is constant along each pipe, this leads to constant friction factors λ^e_{fric} along each pipe. In all examples, the dynamic viscosity is $\eta_v := 11.9{\cdot}10^{-6}\text{kg}\,\text{m}^{-1}\,\text{s}^{-1}$. Note that our analysis does not directly cover the dependency of the friction factor on q^e, but it poses no problems for numerical calculations. For trees, there is no difference between a flow-dependent and a flow-independent friction law. Most of the results presented in this article only rely on the monotonicity property $\partial_{q_e} p^e < 0$ (see Remark 2 for a sufficient condition to ensure this property).

Table 1 contains the constants used for the single pipe computations in Figs. 1 and 2. Table 2 contains the globally used constants and Table 3 the constants for each pipe for the example of a tree networks depicted in Fig. 5. The boundary values for the tree example are presented in Table 4. The globally used constants for the diamond graph (see Figs. 8 and 9) are contained in Table 5. The pipe data for this example is presented in Table 6 and its boundary flow values in Table 7.

TABLE 1
Values for single pipe examples

Symbol	Name	Value	Unit
R	Specific gas constant	448.66	$\text{J}\,\text{kg}^{-1}\,\text{K}^{-1}$
T^e	Temperature	290	K
p_c	Pseudocritical pressure	46.70206	10^5Pa
T_c	Pseudocritical temperature	202.43951	K
α^e	Constant in the state equation	-2.46391	10^{-8}Pa^{-1}
k^e	Roughness	0.06	mm

TABLE 2
Global values for the tree network example

Symbol	Name	Value	Unit
R	Specific gas constant	447.80152	$\text{J}\,\text{kg}^{-1}\,\text{K}^{-1}$
T^e	Temperature	273.15	K
p_c	Pseudocritical pressure	45.92935	10^5Pa
T_c	Pseudocritical temperature	188.54976	K
α^e	Constant in the state equation	-2.41499	10^{-8}Pa^{-1}

TABLE 3
Pipe data for the tree network example

Pipe name	From	To	Length L^e	Diameter D^e	Roughness k^e
pipe_1	source	innode	15.99078 km	1.000 m	0.05 mm
pipe_2	innode	sink_1	44.71898 km	1.000 m	0.05 mm
pipe_3	innode	sink_2	7.05313 km	1.000 m	0.05 mm
pipe_4	innode	sink_3	38.05409 km	1.000 m	0.05 mm

TABLE 4
Given boundary data for the tree network example

Node name	Node outflow b_v	Pressure p_0
source	-130.83333 $\mathrm{kg\,s^{-1}}$	$13.00000 \cdot 10^5$ Pa
innode	0 $\mathrm{kg\,s^{-1}}$	–
sink_i, i=1,...,3	43.61111 $\mathrm{kg\,s^{-1}}$	–

TABLE 5
Global values for the diamond graph example

Symbol	Name	Value	Unit
R	Specific gas constant	460.66628	$\mathrm{J\,kg^{-1}\,K^{-1}}$
T^e	Temperature	288.15	K
p_c	Pseudocritical pressure	46.70206	10^5Pa
T_c	Pseudocritical temperature	202.43951	K
α^e	Constant in the state equation	-2.51506	$10^{-8}\mathrm{Pa^{-1}}$

TABLE 6
Pipe data for the diamond graph example

Pipe name	From	To	Length L^e	Diameter D^e	Roughness k^e
e_1	v_1	v_2	39.74748 km	1.300 m	0.01 mm
e_2	v_2	v_3	37.57120 km	1.000 m	0.01 mm
e_3	v_2	v_4	28.40076 km	1.300 m	0.01 mm
e_4	v_3	v_4	26.59033 km	1.300 m	0.01 mm
e_5	v_3	v_5	17.97404 km	1.000 m	0.01 mm
e_6	v_4	v_5	25.14802 km	1.000 m	0.01 mm
e_7	v_5	v_6	14.58364 km	1.000 m	0.01 mm

TABLE 7
Given boundary data for the diamond graph example

Node name	Node outflow b_v	Pressure p_0
v_1	-453.1495 $\mathrm{kg\,s^{-1}}$	$60 \cdot 10^5$ Pa
v_i, $i = 2, \ldots, 5$	0 $\mathrm{kg\,s^{-1}}$	–
v_6	453.1495 $\mathrm{kg\,s^{-1}}$	–